



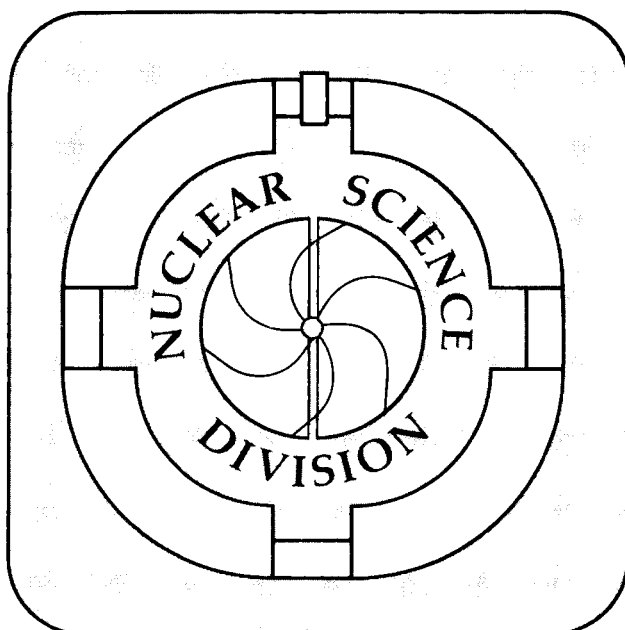
Lawrence Berkeley Laboratory

UNIVERSITY OF CALIFORNIA

RHIC Letter of Intent for An Experiment on Particle and Jet Production at Midrapidity

The STAR Collaboration

September 1990



Prepared for the U.S. Department of Energy under Contract Number DE-AC03-76SF00098

1 LOAN COPY 1
1 Circulates 1
1 for 4 weeks 1
Bldg. 50 Library.
Copy 2

LBL-29651

DISCLAIMER

This document was prepared as an account of work sponsored by the United States Government. While this document is believed to contain correct information, neither the United States Government nor any agency thereof, nor the Regents of the University of California, nor any of their employees, makes any warranty, express or implied, or assumes any legal responsibility for the accuracy, completeness, or usefulness of any information, apparatus, product, or process disclosed, or represents that its use would not infringe privately owned rights. Reference herein to any specific commercial product, process, or service by its trade name, trademark, manufacturer, or otherwise, does not necessarily constitute or imply its endorsement, recommendation, or favoring by the United States Government or any agency thereof, or the Regents of the University of California. The views and opinions of authors expressed herein do not necessarily state or reflect those of the United States Government or any agency thereof or the Regents of the University of California.

An Experiment on Particle and Jet Production at Midrapidity

K. Kadija,¹ G. Paic,¹ D. Vranic,¹ F.P. Brady,² J.E. Draper,² J.L. Romero,² J. Carroll,³
V. Ghazikhanian,³ E. Gulmez,³ G.J. Igo,³ S. Trentalange,³ C. Whitten, Jr.,³ M. Cherney,⁴
W. Heck,⁵ R.E. Renfordt,⁵ D. Röhrich,⁵ R. Stock,⁵ H. Ströbele,⁵ S. Wenig,⁵ T. Hallman,⁶
L. Madansky,⁶ B. Anderson,⁷ D. Keane,⁷ R. Madey,⁷ J. Watson,⁷ F. Bieser,⁸ M.A. Bloomer,⁸
D. Cebra,⁸ W. Christie,⁸ E. Friedlander,⁸ D. Greiner,⁸ C. Gruhn,⁸ J.W. Harris,⁸ H. Huang,⁸
P. Jacobs,⁸ P. Lindstrom,⁸ H. Matis,⁸ C. McParland,⁸ C. Naudet,⁸ G. Odyniec,⁸ D. Olson,⁸
A.M. Poskanzer,⁸ G. Rai,⁸ J. Rasmussen,⁸ H.-G. Ritter,⁸ J. Schambach,⁸ L.S. Schroeder,⁸
P.A. Seidl,⁸ T.J.M. Symons,⁸ S. Tonse,⁸ H. Wieman,⁸ D.D. Carmony,⁹ Y. Choi,⁹
A. Hirsch,⁹ E. Hjort,⁹ N. Porile,⁹ R.P. Scharenberg,⁹ B. Srivastava,⁹ M.L. Tincknell,⁹
A.D. Chacon,¹⁰ K.L. Wolf,¹⁰ W. Dominik,¹¹ M. Gazdzicki,¹¹ W.J. Braithwaite,¹²
J.G. Cramer,¹² D. Prindle,¹² T.A. Trainor,¹² A. Breskin,¹³ R. Chechik,¹³ Z. Fraenkel,¹³
A. Shor,¹³ and I. Tserruya.¹³

This work was supported in part by the Director, Office of Energy Research, Division of Nuclear Physics of the Office of High Energy and Nuclear Physics in the U.S. Department of Energy under contract DE-AC03-76SF00098.

¹ Rudjer Boskovic Institute, 41001 Zagreb, Yugoslavia

² University of California, Davis, California 95616, U.S.A.

³ University of California, Los Angeles, California 90024, U.S.A.

⁴ Creighton University, Omaha, Nebraska 68178, U.S.A.

⁵ University of Frankfurt, D-6000 Frankfurt am Main 90, West Germany

⁶ The Johns Hopkins University, Baltimore, Maryland 21218, U.S.A.

⁷ Kent State University, Kent, Ohio 44242, U.S.A.

⁸ Lawrence Berkeley Laboratory, University of California, Berkeley, California 94720, U.S.A.

⁹ Purdue University, West Lafayette, Indiana 47907, U.S.A.

¹⁰ Texas A & M University, College Station, Texas 77843, U.S.A.

¹¹ Warsaw University, Warsaw, Poland

¹² University of Washington, Seattle, Washington 98195, U.S.A.

¹³ Weizmann Institute of Science, Rehovot 76100, Israel

An Experiment on Particle and Jet Production at Midrapidity

K. Kadija, G. Paic and D. Vranic
Rudjer Boskovic Institute, 41001 Zagreb, Yugoslavia

F.P. Brady, J.E. Draper and J.L. Romero
University of California, Davis, California 95616, U.S.A.

J. Carroll, V. Ghazikhanian, E. Gulmez, G.J. Igo, S. Trentalange and C. Whitten, Jr.
University of California, Los Angeles, California 90024, U.S.A.

M. Cherney
Creighton University, Omaha, Nebraska 68178, U.S.A.

W. Heck, R.E. Renfordt, D. Röhrich, R. Stock, H. Ströbele and S. Wenig
University of Frankfurt, D-6000 Frankfurt am Main 90, West Germany

T. Hallman and L. Madansky
The Johns Hopkins University, Baltimore, Maryland 21218, U.S.A.

B. Anderson, D. Keane, R. Madey and J. Watson
Kent State University, Kent, Ohio 44242, U.S.A.

F. Bieser, M.A. Bloomer, D. Cebra, W. Christie, E. Friedlander, D. Greiner, C. Gruhn,
J.W. Harris, H. Huang, P. Jacobs, P. Lindstrom, H. Matis, C. McParland, C. Naudet,
G. Odyniec, D. Olson, A.M. Poskanzer, G. Rai, J. Rasmussen, H.-G. Ritter,
J. Schambach, L.S. Schroeder, P.A. Seidl, T.J.M. Symons, S. Tonse and H. Wieman
Lawrence Berkeley Laboratory, Berkeley, California 94720, U.S.A.

D.D. Carmony, Y. Choi, A. Hirsch, E. Hjort, N. Porile, R.P. Scharenberg, B. Srivastava
and M.L. Tincknell
Purdue University, West Lafayette, Indiana 47907, U.S.A.

A. D. Chacon and K. L. Wolf
Texas A & M University, College Station, Texas 77843, U.S.A.

W. Dominik and M. Gazdzicki
Warsaw University, Warsaw, Poland

W.J. Braithwaite, J.G. Cramer, D. Prindle and T.A. Trainor
University of Washington, Seattle, Washington 98195, U.S.A.

A. Breskin, R. Chechik, Z. Fraenkel, A. Shor and I. Tserruya
Weizmann Institute of Science, Rehovot 76100, Israel

Overview

The aim of this experiment is to search for signatures of Quark-Gluon Plasma (QGP) formation and investigate the behavior of strongly interacting matter at high energy density. Since there is no single accepted signature for the QGP, it is essential to use a flexible detection system at RHIC that can simultaneously measure many experimental observables. The experiment will utilize two aspects of hadron production that are fundamentally new at RHIC: correlations between *global observables on an event-by-event basis* and the use of *hard scattering of partons* as a probe of the properties of high density nuclear matter. The event-by-event measurement of global observables – such as temperature, flavor composition, collision geometry, reaction dynamics, and energy or entropy density fluctuations – is possible because of the very high charged particle densities, $dn_{ch}/d\eta \approx 1000 - 1500$ expected in nucleus-nucleus collisions at RHIC. Event-by-event fluctuations are expected in the vicinity of a phase change, so experiments must be sensitive to threshold-like features in experimental observables as a function of energy density. Full azimuthal coverage with good particle identification and continuous tracking is required to perform these measurements at momenta where the particle yields are maximal. Measurable jet yields at RHIC will allow investigations of hard QCD processes via both highly segmented calorimetry and high p_t single particle measurements in a tracking system. A systematic study of particle and jet production will be carried out over a range of colliding nuclei from $p + p$ through $Au + Au$, over a range of impact parameters from peripheral to central, and over the range of energies available at RHIC. Correlations between observables will be made on an event-by-event basis to isolate potentially interesting event types. In particular, correlations of jet properties with full event reconstruction may lead to some surprising new physics.

Measurements will be made at midrapidity over a large pseudo-rapidity range ($|\eta| < 1$) with full azimuthal coverage ($\Delta\phi = 2\pi$) and azimuthal symmetry. The detection system will consist of a silicon vertex tracker (SVT) and time projection chamber (TPC) inside a superconducting solenoidal magnet for tracking, momentum analysis and low p_t particle identification via dE/dx ; a time-of-flight system surrounding the TPC for particle identification at higher momenta; and electromagnetic and hadronic calorimetry outside the magnet to trigger on and measure jets, and to measure the transverse energy of events. The tracking and particle identification are needed mainly to study the soft physics, and the calorimetry to study the hard physics. Some of the details of the various detector systems have been worked out, while others require significant research and development before a final design can be established.

I. Physics

The physics goals of the experiment can be divided into two categories: A) the study of soft physics processes, i.e. low p_t hadron production, and B) the study of hard QCD processes, i.e. jet and mini-jet production.

A. Particle Production at Low p_t

The experiment aims to momentum analyze and identify charged particles (π^+ , π^- , K^+ , K^- , p , \bar{p} , d , \bar{d}) directly, as well as various neutral and charged strange particles (K^0_s , ϕ , Λ , $\bar{\Lambda}$, Ξ^- , $\bar{\Xi}^-$) via charged-particle decay modes. A unique feature of this experiment will be its ability to study observables on an event-by-event basis in addition to inclusive measurements. The event-by-event and inclusive measurements that can be made and the physics observables that are studied by these measurements are described below.

Particle Spectra

As a consequence of the high multiplicities in central nucleus-nucleus events, the slope of the transverse momentum (p_t) distribution for pions and the $\langle p_t \rangle$ for pions and kaons can be determined *event-by-event*. Thus, individual events can be characterized by "temperature" to search for events with extremely high temperature, predicted¹ to result from deflagration of a QGP. Displayed in Fig. 1 are two spectra generated by the Monte Carlo method from Maxwell-Boltzmann distributions with $T = 150$ and 250 MeV, each containing 1000 pions. This is the average number of pions of a given charge sign expected in the acceptance $|\eta| < 1$ of this experiment for central Au + Au collisions. The slopes of spectra with $T = 150$ and 250 MeV derived from fits using a Maxwell-Boltzmann distribution, also shown in Fig. 1, can easily be discriminated at the single event level. Fig. 2a shows the standard deviation in measuring $\langle p_t \rangle$ as a function of the charged particle multiplicity measured in a single event. The curves are derived from distributions generated with temperatures of 150 and 250 MeV and are labeled by their corresponding $\langle p_t \rangle$ values. From Fig. 2a it can be seen that the determination of $\langle p_t \rangle$ for pions can be made very accurately on the single event basis in this experiment, over the expected range of multiplicities in central collisions from Ca + Ca to Au + Au. Even for kaons, with ~ 200 charged kaons per event in the acceptance for central Au + Au events, $\langle p_t \rangle$ can be determined accurately for single events.

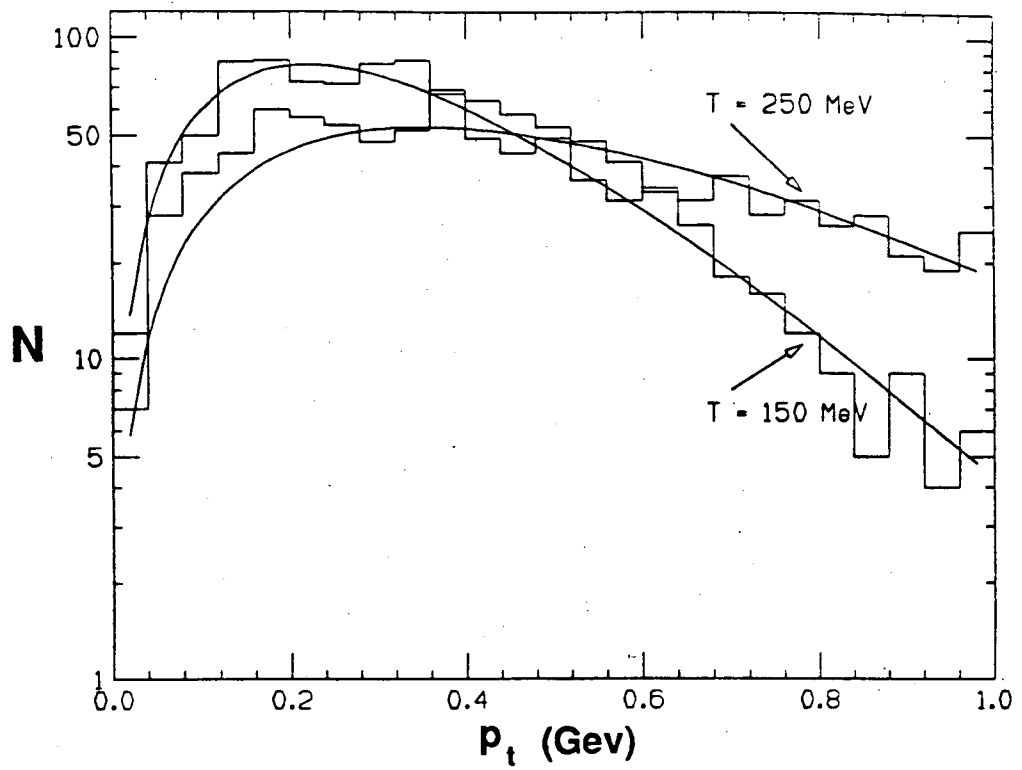
Inclusive p_t distributions of charged particles will be measured with high statistics and effects such as collective radial flow² and critical temperature³ at low p_t , and mini-jet attenuation⁴ at high p_t will be investigated. Comparison of these spectra for pp and AA as a function of impact parameter is important. Large unexplained differences in spectral shapes have been

¹ E.V. Shuryak and O.V. Zhirov, Phys. Lett. B89 (1980) 253; E.V. Shuryak and O.V. Zhirov, Phys. Lett. B171 (1986) 99.

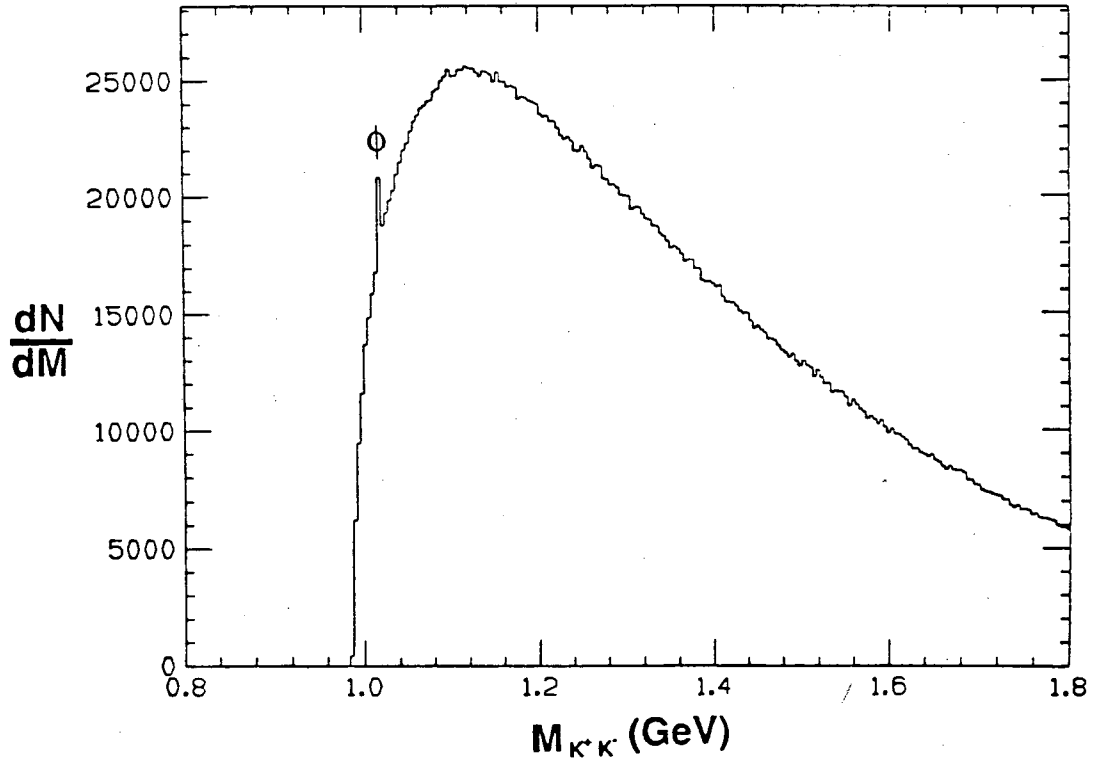
² P.V. Ruuskanen, Z. Phys. C38 (1988) 219.

³ L. Van Hove, Phys. Lett. 118B (1982) 138; K. Redlich and H. Satz, Phys. Rev. D33 (1986) 3747.

⁴ P.V. Landshoff, Nucl. Phys. A498 (1989) 217; X.N. Wang, Lawrence Berkeley Laboratory Report LBL-28790 (1990), submitted to Phys. Rev. D.

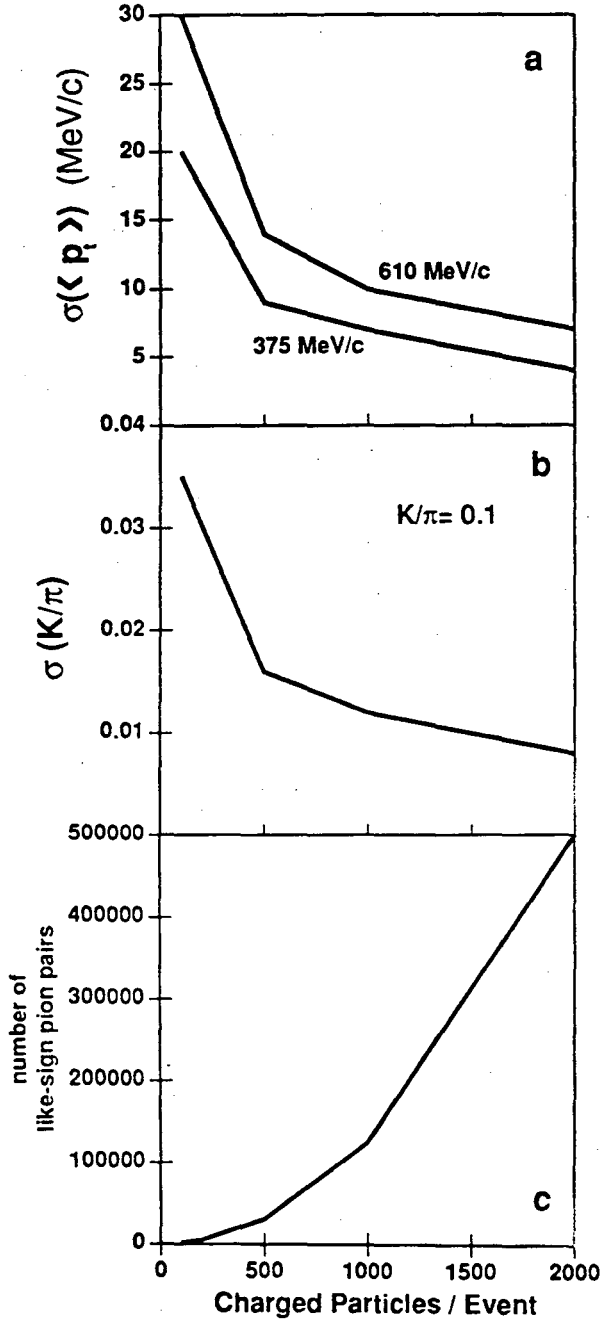


1. Simulation of the p_t spectrum for one event generated using a Boltzmann distribution of 1000 pions. The histograms correspond to single events generated with $T = 150$ MeV and 250 MeV. The curves are fits to the histogram using a Maxwell-Boltzmann distribution (see text).

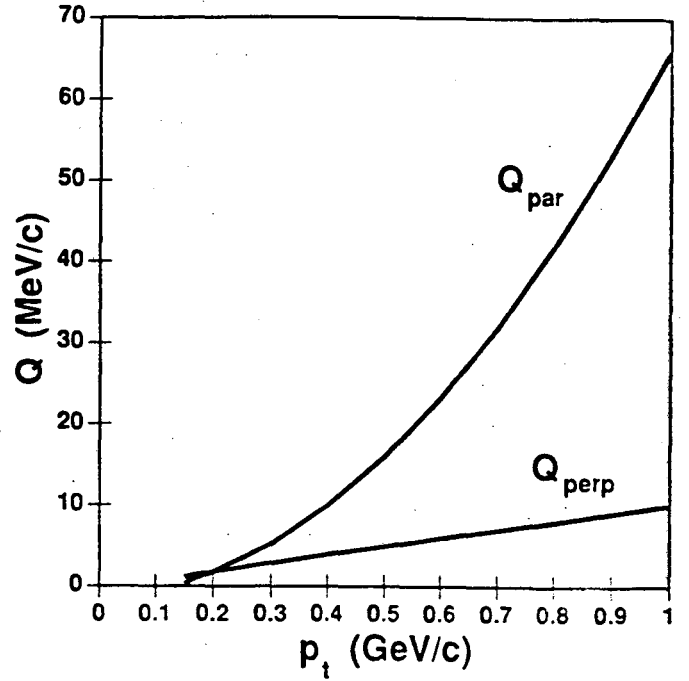


3. Invariant mass distribution for K^+K^- pairs in the acceptance $|\eta| < 1$ for 500 Au + Au central events at RHIC. The ϕ signal is the narrow peak ($\Gamma = 4.4$ MeV) at 1.02 GeV. The mean number of ϕ 's is six per event. The bin size is 4 MeV to correspond to the width of the ϕ although the experimental resolution is expected to be better than this.

Event by Event Physics



2. Plotted as a function of the charged-particle multiplicity measured in an event are a) the standard deviation of $\langle p_t \rangle$, (showing the mean p_t values for temperatures of 150 and 250 MeV) b) the standard deviation of the ratio K/π (assuming $\langle K/\pi \rangle = 0.1$) and c) the number of like-sign pion pairs. A central Au + Au event at RHIC is expected to produce 2000 charged particles (1000 pions of each charge) in the acceptance of this experiment.



4. The magnitude of the momentum difference parallel and transverse to the average momentum vector of a pair of tracks separated by 2 cm at 2 m radius in a 0.5 T magnetic field, as a function of the mean p_t of the pair. The results scale linearly with two-track resolution.

measured in high multiplicity pp, $\alpha\alpha$ and higher mass nucleus-nucleus collisions at the CERN ISR and SPS.^{5,6}

Since the central region of heavy ion collisions at RHIC is expected to have zero net baryon number, the p_t spectra of baryons and anti-baryons at midrapidity are particularly interesting for determining the stopping power of quarks. The difference between the p_t spectra obtained for p and \bar{p} or Λ and $\bar{\Lambda}$ will reflect the redistribution in phase space of valence quarks from the nucleons of the target and projectile. This measurement of the net baryon number and net charge is important for establishing the baryo-chemical potential $\mu_B(y)$ at midrapidity.⁷

Inclusive measurements of multiplicity and the E_t distributions at midrapidity will provide information on the average energy and matter densities, respectively.

Fluctuations in Energy, Entropy, Multiplicity and Transverse Momentum

It has long been known that a prime, general indicator of a phase transition is the appearance of critical dynamical fluctuations in a narrow range of conditions. It is worth emphasizing that such critical fluctuations can only be seen in individual events where the statistics are large enough to overcome uncertainties (\sqrt{N}) due to finite particle number fluctuations. The large transverse energy and multiplicity densities at midrapidity in central collisions allow *event-by-event* measurement of fluctuations in particle ratios, energy density, entropy density and flow of different types of particles as a function of p_t , rapidity, and azimuthal angle. They also allow measurements of local fluctuations in the magnitude and azimuthal distribution of p_t . These fluctuations have been predicted to arise from the process of hadronization of a QGP.⁸

Flavor Composition

One of the first predictions of a signature for the formation of a QGP was the enhancement in the production of strange particles resulting from chemical equilibrium of a system of quarks and gluons⁹. A measurement of the K/π ratio provides information on the relative concentration of strange and nonstrange quarks, i.e. $\langle(s + \bar{s})/(u + \bar{u} + d + \bar{d})\rangle$. This has been suggested¹⁰ as a diagnostic tool to differentiate between a hadronic gas and a QGP, and to study the role of the expansion velocity. The K/π ratio will be measured *event-by-event* with sufficient accuracy to classify the events for correlations with other event observables. This can be seen in Fig. 2b, where the standard deviation of the measured single event K/π ratio is plotted as a function of the charged particle multiplicity measured in the event.

The K/π ratio will be measured very accurately on an *inclusive* basis. It can then be correlated with various observables measured event-by event or on an ensemble basis.

⁵ W. Bell et al., Phys. Lett. 112B (1982) 271; A. Karabarbounis et al., Phys. Lett. 104B (1981) 75; A.L.S. Angelis et al., Phys. Lett. 116B (1982) 379.

⁶ J.W. Harris et al., Nucl. Phys. A498 (1989) 133c.

⁷ R. Anishetty, P. Koehler and L. McLerran, Phys. Rev. D22 (1980) 2793; W. Busza and A.S. Goldhaber, Phys. Lett. 139B (1984) 235; S. Date, M. Gyulassy and H. Sumiyoshi, Phys. Rev. D32 (1985) 619.

⁸ M. Gyulassy, Nucl. Phys. A400 (1983) 31c; L. Van Hove, Z. Phys. C27 (1985) 135.

⁹ R. Hagedorn and J. Rafelski, Phys. Lett. 97B (1980) 180; J. Rafelski and B. Mueller, Phys. Rev. Lett. 48 (1982) 1066; P. Koch, B. Mueller and J. Rafelski, Phys. Rep. 142 (1986) 167.

¹⁰ N.K. Glendenning and J. Rafelski, Phys. Rev. C31 (1985) 823; K.S. Lee, M.J. Rhoades-Brown and U. Heinz, Phys. Rev. C37 (1988) 1452.

The production cross section of ϕ -mesons can be measured *inclusively* from the decay $\phi \Rightarrow K^+ + K^-$. Displayed in Fig. 3 is an invariant mass spectrum, in the region of the ϕ mass, constructed from all possible combinations of K^+ and K^- in the acceptance $|\eta| < 1$. Measurement of the yield of the ϕ , which is an $s\bar{s}$ pair, places a more stringent constraint on the origin of the observed flavor composition¹¹ than the K/π ratio and is expected to be more sensitive to the presence of a QGP. The ϕ production rate is also expected to be extremely sensitive to changes in the quark masses^{12,13} due to a chiral phase transition at high energy densities, which is predicted in lattice QCD calculations.^{14,15}

Measurement of the multiplicities of Λ , $\bar{\Lambda}$ and multiply-strange baryons provides a better determination of the strange/nonstrange quark ratio than do the K/π ratios. Like the ϕ , multiply-strange baryons are sensitive to the existence of a QGP,¹⁶ more so than singly-strange particles. However, their observation requires detection of secondary decay vertices. Due to the short decay lengths, $c\tau \sim 2 - 8$ cm, a silicon vertex tracker (SVT) close to the beam axis is necessary for these measurements.

A measurement of the predicted QGP enhancement of "open charm", e.g. the yield of D-mesons, would be of extreme interest.¹⁷ The ability to measure the D-meson will depend upon developments in silicon vertex tracking in the RHIC environment. This is currently the focus of computer simulations and a RHIC R&D proposal.

Particle Correlations (Bose-Einstein and Speckle Interferometry)

Correlations between identical bosons provide information on the freezeout geometry,¹⁸ the expansion dynamics¹⁹ and possibly the existence of a QGP.²⁰ It would be interesting and unprecedented to be able to measure the pion source parameters via pion correlation analysis on an *event-by-event* basis and to correlate them with other event observables. In an individual event with 1000 negative pions, the number of $\pi^-\pi^-$ pairs within $|\eta| < 1$ is $n_{\pi^-}(n_{\pi^-}-1)/2 = 500,000$. The dependence of the number of like-sign pion pairs on the charged particle multiplicity per event is shown in Fig. 2c. The two-pion correlation statistics for a single central Au + Au event at RHIC will be similar to the accumulated statistics published in most papers on the subject. However, it is necessary to determine precisely the statistics of the correlation function expected in the Bose-Einstein enhancement region of small momentum difference Q , as a function of multiplicity density. An empirical relation for the transverse radius (R_t) of the pion source at midrapidity as a function of the rapidity density (dn/dy) has been derived from existing

¹¹ A. Shor, Phys. Rev. Lett. 54 (1985) 1122.

¹² R. D. Pisarski and F. Wilczek, Phys. Rev. D29 (1984) 338.

¹³ T. Hatsuda and T. Kunihiro, Phys. Lett. B185 (1987) 304.

¹⁴ C.E. DeTar and J.B. Kogut, Phys. Rev. Lett. 59 (1987) 399; Phys. Rev. D36 (1987) 2828.

¹⁵ E.V.E. Kovacs et al., Phys. Rev. Lett. 58 (1987) 751; F. Karsch et al., Phys. Lett. 188B (1987) 353.

¹⁶ J. Rafelski, Phys. Rep. 88 (1982) 331.

¹⁷ T. Matsui and H. Satz, Phys. Lett. 178B (1986) 416.

¹⁸ F.B. Yano and S.E. Koonin, Phys. Lett. B78 (1978) 556; K. Kolehmainen and M. Gyulassy, Phys. Lett. B180 (1986) 203; B. Andersson and W. Hofmann, Phys. Lett. B169 (1986) 364.

¹⁹ A. Bamberger et al., Phys. Lett. B203 (1988) 320.

²⁰ S. Pratt, Phys. Rev. D33 (1986) 1314; G. Bertsch, M. Gong and M. Tohyama, Phys. Rev. C37 (1988) 1896 and G. Bertsch MSU Preprint (1988).

pion correlation data.²¹ This relation, $R_t \sim \sqrt{(dn/dy)}$, suggests rather large source sizes, $R_t \sim 20 - 30$ fm, for central Au + Au collisions at RHIC. Such large source sizes would confine the two-pion correlation enhancement to small values of $Q < 6 - 10$ MeV/c. An extrapolation of the CERN NA35 two-pion correlation data¹⁹ to central Au + Au collisions at RHIC suggests that more than adequate statistics will be available at small Q for these large source sizes on an event-by-event basis. However, the necessity to accurately measure small values of Q places stringent constraints on the two-track resolution of the tracking system. Displayed in Fig. 4 is the minimum Q which can be observed as a function of the average p_t of the pair of tracks for a two-track resolution of 2 cm at 2 m distance from the interaction vertex. For an expected pion $\langle p_t \rangle \sim 300 - 400$ MeV/c, a Q of 3 MeV/c could be measured in the transverse (space) direction, but not in the parallel (time) direction. The two-track resolution necessary for distinguishing identical pairs is independent of the particle species.

Three, four and higher particle number correlations can also be analyzed²², in addition to two particle correlations. With the high pion density in phase space, unique to RHIC, a novel aspect of multi-pion clustering, analogous to optical speckle interferometry,²³ should be observable for the first time.²⁴ These "speckles" are a collective multi-particle effect which leads to large scale structure in phase space. They may offer information on the hadronic source which is complementary to that deduced from traditional Bose-Einstein pair correlation analysis. However, interpretation of higher order particle correlations and "speckle interferometry" data requires significant theoretical progress, in particular on Coulomb multiparticle corrections.

The correlations of like-sign charged kaons or pions will be measured on an *inclusive* basis to high accuracy. The dependence of the source parameters on the transverse momentum components of the particle pairs will be measured with high statistics. Measurement of correlations between unlike-sign pairs will yield information on the Coulomb corrections and effects of final state interactions, which must be taken into consideration to interpret the like-sign pair distributions. This is important since the Coulomb corrections may also depend upon the spacetime evolution of the source.

The *inclusive* measurement of KK correlations will complement the $\pi\pi$ correlation data. The KK correlation is less affected by resonance decays after hadronic freeze-out than the $\pi\pi$ correlations²⁵, thus interpretation of the KK correlation measurements is much less model-dependent than that of the $\pi\pi$ data. Since K's are expected to freeze out earlier²⁶ than π 's in the expansion, the K source sizes are expected to be smaller than those of the π 's, resulting in less stringent constraints on the two-track resolution of the tracking system. Depending upon the baryo-chemical potential and the existence of a QGP, the K^+ and K^- are also expected to freeze out at different times.²⁶ Thus, separate measurements of the K^+K^+ and K^-K^- correlation functions will be of interest.

²¹ R. Stock, University of Frankfurt Preprint IKF90-3 (1990), to be published in Annalen der Physik.

²² Y.M. Liu et al., Phys. Rev. C **34**, (1986) 1667.

²³ A. Labeyrie in Progress in Optics, ed. E. Wolf, North-Holland Publishing Co., Amsterdam Vol. 14 (1976).

²⁴ W.A. Zajc, Phys. Rev. D **35** (1987) 3396.

²⁵ M. Gyulassy and S. S. Padula, Lawrence Berkeley Laboratory Report LBL-26077 (1988).

²⁶ K.S Lee, M.J. Rhoades-Brown and U. Heinz, Phys. Rev. C **37** (1988) 1463.

Expansion Dynamics

Anti-deuterons and heavier anti-nuclei result from the coalescence of combinations of \bar{p} and \bar{n} during expansion, when the anti-nucleon density reaches freezeout density. The "coalescence ratio" $\langle \bar{d} \rangle / \langle \bar{p} \rangle^2$ depends not only on the dynamics of source expansion (radial flow, temperature, etc.) at freezeout, but also on the source size. This ratio decreases with increasing source radius, and should provide information complementary to the particle correlation analyses.²⁷ In a region of zero net baryon number, deuterons will also serve the same purpose.

B. Products of Hard QCD Processes

The goal of studying products of hard QCD processes produced in relativistic heavy ion collisions is to use the propagation of quarks and gluons as a probe of nuclear matter, hot hadronic matter and quark matter. Since the hard scattering processes are directly calculable in QCD, a measurement of the yield of hard scattered partons as a function of their transverse energy should be sensitive to their interaction with the surrounding matter. Various calculations have predicted that the propagation of quarks and gluons depends strongly upon properties of the medium.^{28,29,30,31,32} A comparison of the measured yield as a function of energy of the products of hard QCD scattering processes in pp, pA and AA collisions, together with theoretical predictions for parton propagation through nuclear, hadronic and quark matter, will furnish valuable information on the composition of the matter in these collisions.

Jets

Hard parton-parton collisions will occur within the first fm/c of the start of the nucleus-nucleus collision.^{33,34} Hence, the partons in a single hard scattering (dijet) whose products are observed at midrapidity must traverse distances of several fermi through high density matter in a nucleus-nucleus collision. The energy loss of these propagating quarks and gluons is predicted^{32,35} to be sensitive to the medium and may be a direct method of observing the excitation of the medium, i.e., the QGP. Passage through hadronic or nuclear matter is predicted to result in an attenuation of the jet energy and broadening of jets. Relative to this damped case, a QGP is transparent and an enhanced yield is expected. The yield of jets will be measured as a function of the transverse energy of the jet. The jet events can also be correlated with other *event-by-event* observables to deduce information on the dynamics of the collision process. The jet

²⁷ S. Mrowczynski, Regensburg Report (1990) to be published in Phys. Lett.

²⁸ J.D. Bjorken, Fermilab Report 82/59/59-THY (1982).

²⁹ D. Appel, Phys. Rev. D33 (1986) 717.

³⁰ J.P. Blaizot and L.D. McLerran, Phys. Rev. D34 (1986) 2739.

³¹ M. Rammersdorfer and U. Heinz, Phys. Rev. D41 (1990) 306.

³² M. Gyulassy and M. Plummer, Phys. Lett. B243 (1990) 432.

³³ E.V. Shuryak in Proceedings of the Workshop on Experiments and Detectors for RHIC, Brookhaven National Laboratory, Upton, New York, 2-7 July 1990 to appear as a BNL report.

³⁴ T. Matsui in Proceedings of the Workshop on Experiments and Detectors for RHIC, Brookhaven National Laboratory, Upton, New York, 2-7 July 1990 to appear as a BNL report.

³⁵ X.N. Wang and M. Gyulassy in Proceedings of the Workshop on Experiments and Detectors for RHIC, Brookhaven National Laboratory, Upton, New York, 2-7 July 1990 to appear as a BNL report.

studies require systematic measurements of pp interactions in addition to heavier mass systems. Systematics as a function of impact parameter for heavier systems are particularly important. The pA systems will also be studied to measure the degree to which jets are quenched in traversing cold nuclear matter.

Wang and Gyulassy have developed a model³⁵ to simulate nucleus-nucleus collisions at RHIC using as a basis the Pythia model³⁶ for pp interactions and including of the nucleus-nucleus geometry. Partons are propagated through matter in the collision and their energy loss is calculated depending upon the type of matter traversed (nuclear, hadronic or QGP). Results from these simulations exhibit a strong attenuation of jets and mini-jets in hadronic matter. The attenuation disappears for traversal of deconfined matter (QGP). The results of the calculations are very much dependent upon the dynamics of the collisions, and the effects are largest at midrapidity. A detailed study of the effects of mini-jet and jet attenuation on the transverse energy is underway.

It is essential to measure the energy of both jets in dijet events. The sum of the jet energies and the dijet invariant mass are sensitive to interactions of the partons with the medium. The yield as a function of invariant mass of back-to-back jets at midrapidity may be the best tool for studying effects of the matter on propagation, since in this case the overall path length in the medium is maximized. The difference of dijet energies is sensitive to the difference in path lengths traversed by the partons. In addition, measurement of both jets in a dijet event suppresses background due to fluctuations of soft production processes that can mimic a jet. A measurement of the dijet differential cross section for nucleus-nucleus collisions will in itself be of interest for understanding the parton structure functions in nuclear matter.

Mini-Jets and High p_t Tails of Distributions

Mini-jets are expected to be produced copiously in collisions at RHIC.^{37,38} As is the case for high p_t jets, the observed yield of mini-jets is expected to be influenced strongly by the state of the high density medium through which they propagate.⁴ However, direct measurement of mini-jets is virtually impossible because of their large opening angle and the strongly varying background. Thus, it is important to study the degree of fluctuation of the transverse energy and multiplicity as a function of rapidity and azimuthal angle ($d^2E_T/dy d\phi$ and $d^2n/dy d\phi$) *event-by-event*, which should be strongly affected by the mini-jets.^{35,39} It is essential that this be systematically studied in pp and pA collisions, as well as AA.

Inclusive p_t distributions of hadrons at $p_t > 3$ GeV/c will also be influenced by jets and mini-jets. However, it should be emphasized that the single particle cross sections fall off more rapidly as a function of p_t than the jet cross sections.⁴⁰ Furthermore, accurate determination of jet energies from the momentum of leading particle which are products of jet fragmentation,⁴⁰ cannot be made on an event-by-event basis.

³⁶ T. Sjostrand and M. van Zijl, Phys. Rev. D36 (1987) 2019.

³⁷ K. Kajantie, P.V. Landshoff and J. Lindfors, Phys. Rev. Lett. 59 (1987) 2527.

³⁸ K.J. Eskola, K. Kajantie and J. Lindfors, Nucl. Phys. B323 (1989) 37.

³⁹ X.N. Wang, Lawrence Berkeley Laboratory Report LBL-28789 (1990), submitted to Phys. Lett. B.

⁴⁰ see W. Geist et al., CERN/EP Report 89-159 (1989) to be published in Phys. Rep. (1990).

Di-quarks at High p_t

The formation and attenuation rates of subhadronic objects, such as di-quarks, will also depend upon the state of the medium.⁴¹ Although little theoretical consideration has been given to this subject, an investigation of di-quark scattering and attenuation at high p_t and production of Λ and $\bar{\Lambda}$ at high p_t should provide interesting information on this issue.

C. Correlations between Event Observables

It should be emphasized that the capability of measuring several different observables event-by-event is unique to this experiment. Events can be characterized event-by-event by their temperature, flavor content, transverse energy density, multiplicity density, entropy density, degree of fluctuations, occurrence of jets and possibly source size. The presence of a QGP is not likely to be observed in an average event, nor is it expected to be observed in a large fraction of events. Since there is no single clearly established signature of the QGP, access to many observables simultaneously will be critical for identifying the rare events in which a QGP is formed.

II. Detecting and Measuring Jets at RHIC

Jets in high energy collisions have been studied in two ways. One technique involves triggering on single high p_t hadrons (leading particles of jets) and studying the associated soft charged particles.^{42,43} Leading particles of jets approximate well the direction of the jet. The fraction of the jet momentum taken by the leading particle can be well determined on the average.^{42,43} However, this fraction fluctuates event-by-event by approximately 30% about the mean,⁴⁴ as dictated by the fragmentation function. Therefore, the jet energy cannot be well determined by leading particles on an event-by-event basis. Another method uses calorimetry to integrate over the entire p_t spectrum, including neutral particles, and measures the full jet energy event-by-event.⁴⁵ At RHIC, the presence of a large number of soft particles in a central Au + Au event presents a problem for studying jets through calorimetry. These particles create a fluctuating background of energy in each calorimeter module which determines a lower limit on the E_t at which the jet can be found and also limits the resolution to which the jet energy can be determined event-by-event. These points will be discussed in more detail below.

In this experiment both techniques will be utilized: calorimetry for high E_t jets (with the lower limit on E_t yet to be established, but at least greater than 20 GeV) and leading charged hadrons analyzed in the TPC for jets with $E_t < 15$ GeV. The leading particle spectrum falls faster than the jet spectrum⁴⁶ as a function of p_t , so that single particle studies are restricted to lower p_t due to rate. In addition to the many event-by-event observables of soft particles in this experiment, a detailed measurement of jet events will be made at RHIC. This will allow correlations between the hard and soft physics and provide a complete picture of the event.

⁴¹ W. Geist, Phys. Lett. B211 (1988) 233.

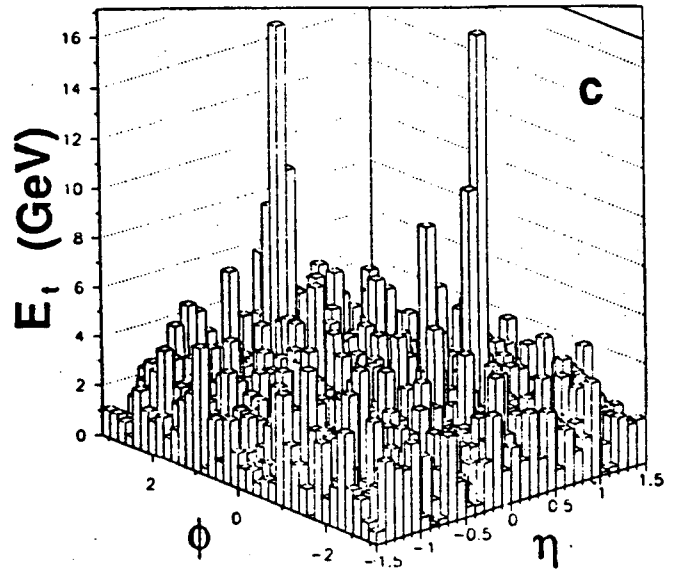
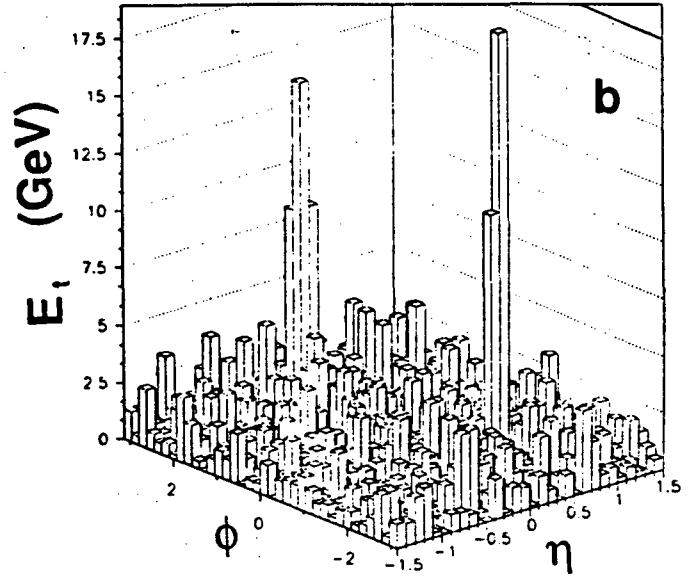
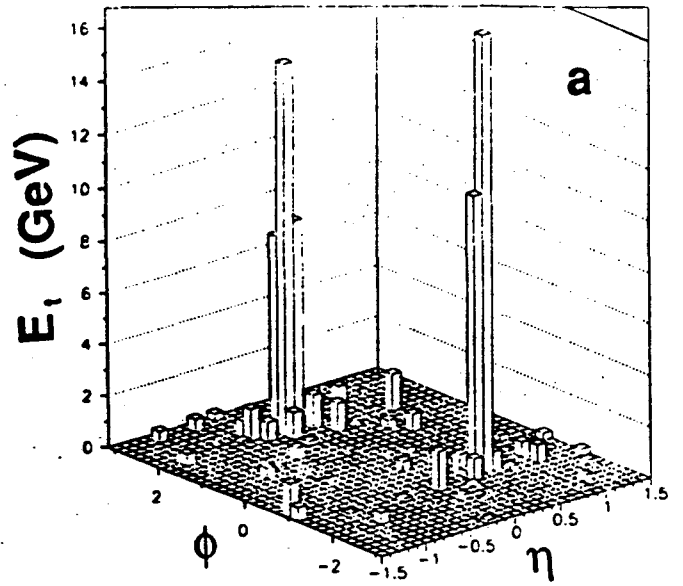
⁴² A. Breakstone et al., Z. Phys. C23 (1984) 9.

⁴³ A.L.S. Angelis et al., Nucl. Phys. B209 (1982) 284.

⁴⁴ C.D. Buchanan, Proc. XVIIth Rencontre de Moriond, Les Arcs, France, vol. II (1982) 139.

⁴⁵ L. DiLella, Ann. Rev. Nucl. Part. Sci. 35 (1985) 107.

⁴⁶ A. Breakstone et al., Phys. Lett. 135B (1984) 505.



5. a) A plot of E_t vs ϕ and η of a 40 GeV dijet event generated by Isajet for a $\sqrt{s} = 200$ GeV pp collision. b) A plot of E_t vs ϕ and η for the same hard parton-parton scattering mixed into a $\sqrt{s} = 200$ GeV/n Au + Au event, generated at impact parameter $b = 5.5$ fm by the Lund/Fritiof nucleus-nucleus code. c) The same for a $b = 0$ Au+Au event. A lateral segmentation of $\Delta\phi = 10^\circ$ and $\Delta\eta = 0.1$ for the calorimetry is assumed. No effects of detector resolution have been input into this calculation.

The jet production rates at RHIC have been calculated.⁴⁷ For Au ions at a $\sqrt{s} = 200$ GeV/n and a luminosity of $2 \times 10^{26} \text{ cm}^{-2}\text{sec}^{-1}$, the expected singles rates for jets are approximately 4×10^4 , 26, and 0.08 per day for $p_t > 20$, 40 and 60 GeV/c, respectively. These rates are independent of the mass of the beam at RHIC because the parton-parton luminosity is roughly independent of the beam mass.

Various methods of generating jet events, studying properties of jets, and measuring jets in nucleus-nucleus collisions at RHIC have been investigated. Displayed in Fig. 5a is a 40 GeV dijet event generated by Isajet⁴⁸ for a $\sqrt{s} = 200$ GeV pp collision as viewed by the calorimeters in E_t vs ϕ and η space. The two jets are identified easily and their energies and directions measured. Fig. 5b and c show the same hard parton-parton scattering mixed into $\sqrt{s} = 200$ GeV/n Au + Au events, generated by the Lund/Fritiof nucleus-nucleus code⁴⁹ at impact parameters of $b = 5.5$ fm and $b = 0$. Jets are qualitatively more difficult to find and measure in the background of a central Au + Au event. The CDF jet-finding algorithm⁵⁰ was used to study the feasibility of identifying and measuring jets in collisions at RHIC. The results are summarized in Fig. 6. Displayed in Fig. 6a are the efficiencies for finding one and both jets of a pair in the background of a central Au + Au collision as a function of the E_t of the jet. The efficiencies increase as the E_t of the jet increases. Displayed in Fig. 6b is the measured E_t of the jet as a function of the E_t of the jet known from the simulation. The jet E_t is extracted by subtraction of the underlying average background in the region of the jet determined by the jet-finder. The error bars shown in Fig. 6b are the standard deviations of the measurements, without effects of detector resolution. Displayed in Fig. 6c are the standard deviations for determination of ϕ , η , and E_t for jets in the simulations. The jet energies can be determined well on the average, but fluctuations of the background increase the error in the measurements over those measured in pp interactions. Precise determination of E_t is critical because of the steeply falling jet cross section as a function of jet E_t . Determination of the jet direction is affected less by the background and the accuracy is less important than the jet E_t determination.

Effects on the jet energy resolution of momentum cutoffs due to the magnetic field and division of the measured energy into electromagnetic and hadronic fractions have been investigated using the Pythia simulation code. These calculations indicate that determination of electromagnetic or hadronic energy alone is insufficient for accurate jet energy determination event-by-event, due mainly to the low particle statistics (10-15) in the jet. The primary source of fluctuations of the background are mini-jets.

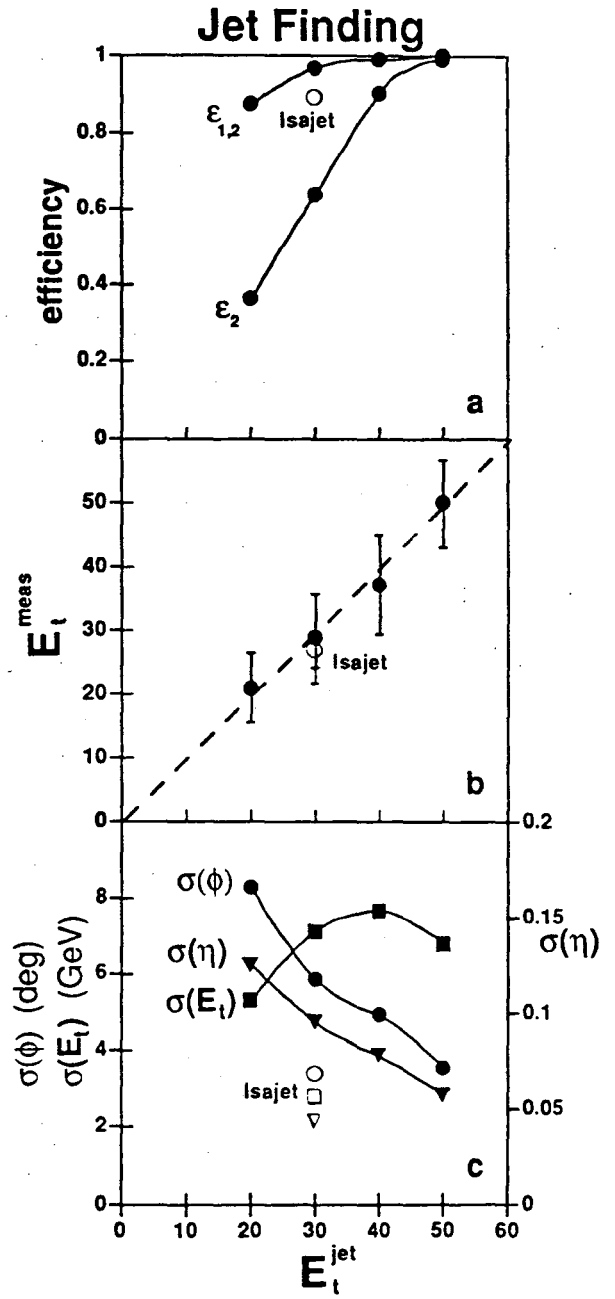
Perhaps the most complicated and most important effect is that of misidentifying fluctuations of the soft and semi-soft (mini-jet) background as jets. Single towers with large values of E_t are the most likely candidates of the "false jets" that can arise from background fluctuations. Preliminary simulations indicate that simple criteria, such as a single tower exceeding a certain value of E_t , will not be sufficient to discriminate between true jet events and "false" jet events, at least not for central Au+Au collisions. Innovative jet-finding algorithms which are qualitatively different from those used currently in pp collider experiments are necessary for the unique

⁴⁷ T. Ludlam, L. Madansky and F. Paige, Proc. of LBL Workshop on detectors for Relativistic Nuclear Collisions, ed. L.S. Schroeder, Lawrence Berkeley Laboratory Report LBL-18225 (1984) 115.

⁴⁸ F.E. Paige and S.D. Protopopescu, ISAJET, Brookhaven National Laboratory Report BNL-37066 (1985).

⁴⁹ B. Andersson et al., Nucl. Phys. B281 (1987) 289. B. Nilsson-Almqvist and E. Stenlund, Comput. Phys. Commun. 43 (1987) 387.

⁵⁰ F. Abe et al., Phys. Rev. Lett. 62 (1989) 613.



6. a) The efficiency for finding dijets in a simulation using the CDF jet-finding algorithm plotted as a function of the transverse energy E_t of the jet. A lateral segmentation of $\Delta\phi = 10^\circ$ and $\Delta\eta = 0.1$ of the calorimeters was used. The 400 events were generated using the Lund/Fritiof model for $\sqrt{s} = 200$ GeV/n Au + Au at impact parameter $b=0$ and superimposing dijets generated with Isajet at the same incident energy. Plotted are the efficiencies for finding one jet of the pair $\epsilon_{1,2}$ and both jets of the pair ϵ_2 . Also plotted is a point for the efficiency for finding jets in a pp event with the same code. b) The measured transverse energy E_t of the jet as a function of the actual transverse energy E_t of the jet for the same sample of events. c) The standard deviations in determining the azimuthal angle ϕ , pseudorapidity η and transverse energy E_t of the jet as a function of the jet transverse energy E_t .

environment of RHIC. Such algorithms will have to exploit more fully the characteristic topologies of dijet events, such as requiring roughly back-to-back large E_t towers. Furthermore, careful design of the calorimetry is necessary to improve the jet energy signal/background. The problem of background jets requires further investigation.

III. Layout of Experiment

A. Design Criteria of Experiment

The physics goals require a large acceptance device having the capability of measuring simultaneously many different observables, representing both soft and hard physics. The design criteria to measure both soft ($p_t < 1.5$ GeV/c) and hard physics (single particles with $p_t > 1.5$ GeV/c and jets) observables are given below:

Soft Physics

- Detection of as many charged particles as possible for $p_t < 1.5$ GeV/c, to provide high statistics for event-by-event observables and fluctuation studies
- Good tracking efficiency as close to the vertex as possible, to contain the size and cost of the experiment
- Particle identification for $p_t < 1.5$ GeV/c
- High kaon detection efficiency for event-by-event observables and for inclusive measurement of the ϕ
- Momentum resolution $\Delta p/p < 0.01$ for $p_t < 1.5$ GeV/c for HBT correlation studies
- Two-track resolution providing a momentum difference, Q , resolution of a few MeV/c for HBT correlation studies
- Accurate determination of the primary vertex to give high momentum resolution
- Accurate determination of secondary vertices for detecting Λ 's and other long-lived particles and resonances

Hard Physics

- Large uniform acceptance to maximize rates, minimize edge effects in jet reconstruction, and measure dijets
- Calorimetry for high E_t jets, tracking with good momentum resolution up to $p_t = 10$ GeV/c for leading charged particles in jets
- 2π azimuthal coverage of calorimetry for event characterization
- Linear response of calorimetry for accurate energy measurements
- Calorimetry segmentation which is an order of magnitude finer than the typical jet size, radius $r = \sqrt{(d\eta^2 + d\phi^2)} \sim 1$

Thus, the physics goals dictate the design of this experiment. To meet these design criteria the experiment will consist of tracking, particle identification and calorimetry at midrapidity over a large pseudorapidity range ($|\eta| < 1$) with full azimuthal coverage ($\Delta\phi = 2\pi$) and azimuthal symmetry. The tracking system will consist of a silicon vertex tracker (SVT) to locate the primary and secondary vertices and a time projection chamber (TPC) inside a solenoidal magnet for *continuous* tracking, optimum momentum resolution and particle identification. A time-of-flight (TOF) system will surround the TPC to extend particle identification to higher momenta than achievable using dE/dx alone. Electromagnetic and hadronic calorimetry will be used to

measure and trigger on jets and the transverse energy of events. A diagram of the experiment is shown in Fig. 7.

Momentum analysis and particle identification of almost all charged particles at midrapidity are necessary. The tracking should operate in conditions at higher than the expected maximum charged particle multiplicities ($n_{ch} = 3000$ in the $|\eta| < 1$ acceptance of the experiment) for central Au + Au collisions. Particle identification of pions/kaons/protons at $p < 2 - 3$ GeV/c and measurement of decay particles from secondary vertices will be possible. The particle identification via TOF for two-particle correlation analysis requires much higher segmentation of the TOF than for identification of single tracks. At present, a two-track resolution of 2 cm at 2 m radial distance from the interaction is envisioned. Momentum resolution of $\Delta p/p < 0.01$ at $p = 0.1$ GeV/c is required by two-particle correlations, and $\Delta p/p$ of a few percent at $p = 10$ GeV/c is necessary to accurately measure spectra at high p_t and particles from mini-jets and jets. It is anticipated that the momentum resolution for high p_t can be improved by further design, optimization and integration of the silicon vertex tracker (SVT). The momentum resolution at low p_t is limited by multiple scattering. To minimize multiple scattering and photon conversion after π^0 decay, which also creates non-primary vertex tracks, detector material will be kept at a minimum throughout the tracking system. A list of the expected materials, thicknesses, and radiation and interaction lengths can be found in Appendix 1.

B. Magnetic Field

Table 1. Magnet Properties	
Solenoid field	0.5 T
Length	8 m
Superconducting coil	
Radius	2 m
Thickness	$< 0.5 L_r$
Yoke	
Radius	4 m
Thickness	12.5 cm Fe
Weight	197 tons
Pole tips	
Max. thickness	25 cm Fe
Weight of each	66 tons
Total weight of Fe	329 tons

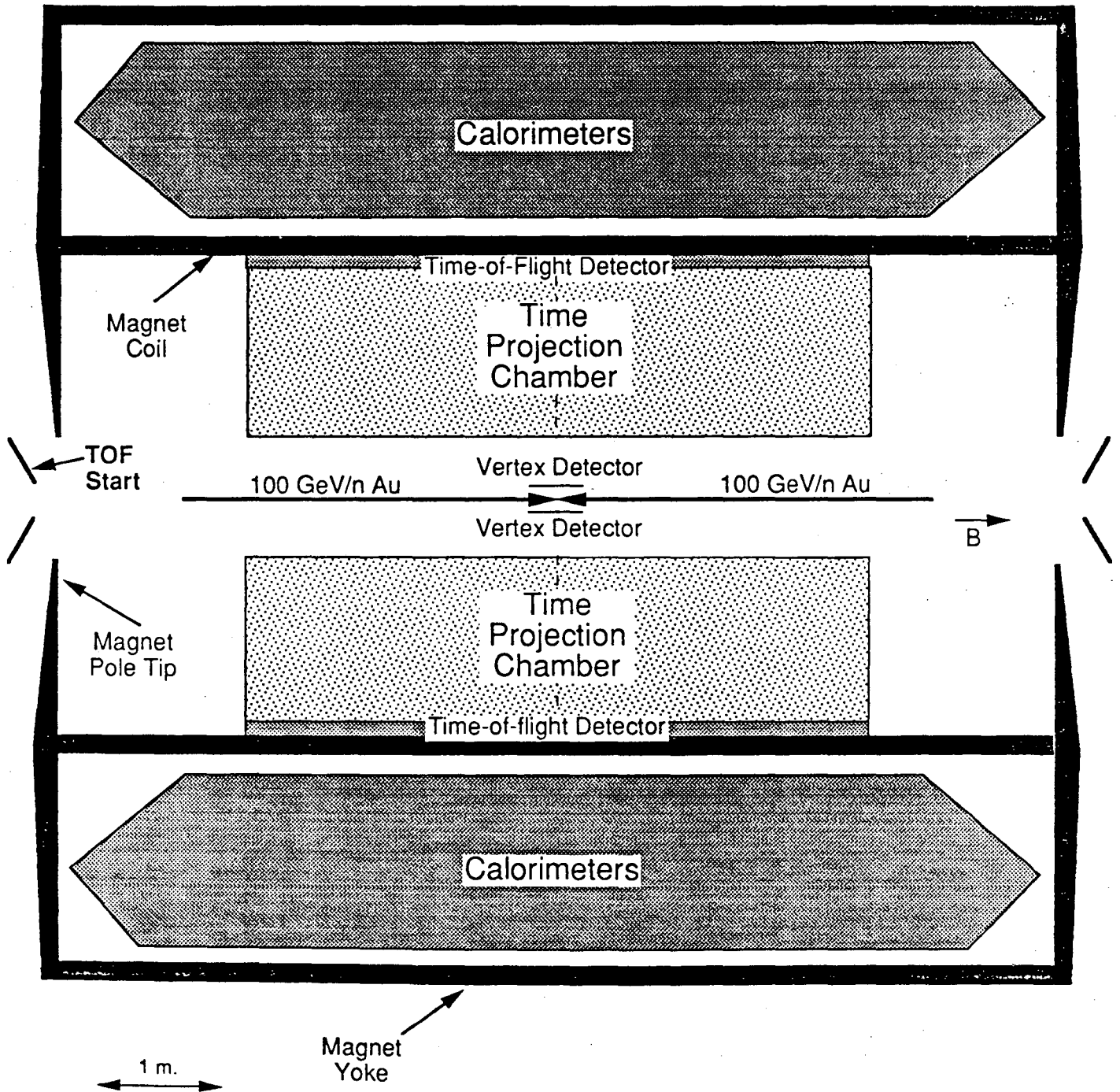
The magnet will be a solenoid with uniform magnetic field along the beam direction. This magnet design is chosen for high tracking accuracy and azimuthal symmetry. A field strength of 0.5 Tesla will provide adequate resolution for momenta as high as 10 GeV/c with only modest spiralling of low p_t particles. With a TPC inner radius of 0.5 m the acceptance will extend to transverse momenta as low as 40 MeV/c. The magnetic coil radius will be 2 m and the radius of the yoke 4 m. Both are 8 m in length. A room temperature Al coil would be too thick to do electromagnetic calorimetry behind it and the power costs would be too high. These two points dictate that the magnet be a superconducting solenoid. It is expected that such a low field superconducting coil and

cryostat can be made less than 0.5 radiation lengths thick. Of course the power usage will be small. Even for this size superconducting magnet the estimated costs are rather moderate because of the low field and the simple design of the yoke and pole-tips.

C. Time Projection Chamber (TPC)

The TPC will consist of two sections, each 2.5 m long, as shown in Fig. 7. The electrons will drift to two end-caps, located on the outer ends. Each end-cap is instrumented with 75,000 pads, each of dimension 8 mm x 20 mm. Each pad collects the charge and generates 512 time samples. Singly-charged particles with $p_t < 40$ MeV/c spiral inside the TPC inner radius of 50

RHIC Experiment on Particle and Jet Production



7. Conceptual layout of the experiment, with cylindrical symmetry around the beam axis. See text for description.

cm and do not reach the TPC. Particles with $40 \text{ MeV}/c < p_t < 150 \text{ MeV}/c$ spiral inside the TPC and most exit the end-caps. Particles with $p_t > 150 \text{ MeV}/c$ traverse the TPC and exit the outer edge at radius 200 cm. The TPC acceptance for particles reaching the outer radius (i.e. with full dE/dx measurement and tracking) is $|\eta| < 1$ and that for particles reaching the inner radius (i.e. multiplicity with partial dE/dx and tracking) is $|\eta| < 1.7$. Details of the TPC design can be found in Table 2.

Table 2. Time Projection Chamber	
Sections	2
Inner radius	0.5 m
Outer radius	2.0 m
Length of each section	2.5 m
# pads at each of 2 endcaps	75,000
Pad size	8 mm x 20 mm
Tracking accuracy	100 μm
Two-track resolution	2 cm
Time samples	512
Drift time	50 μsec

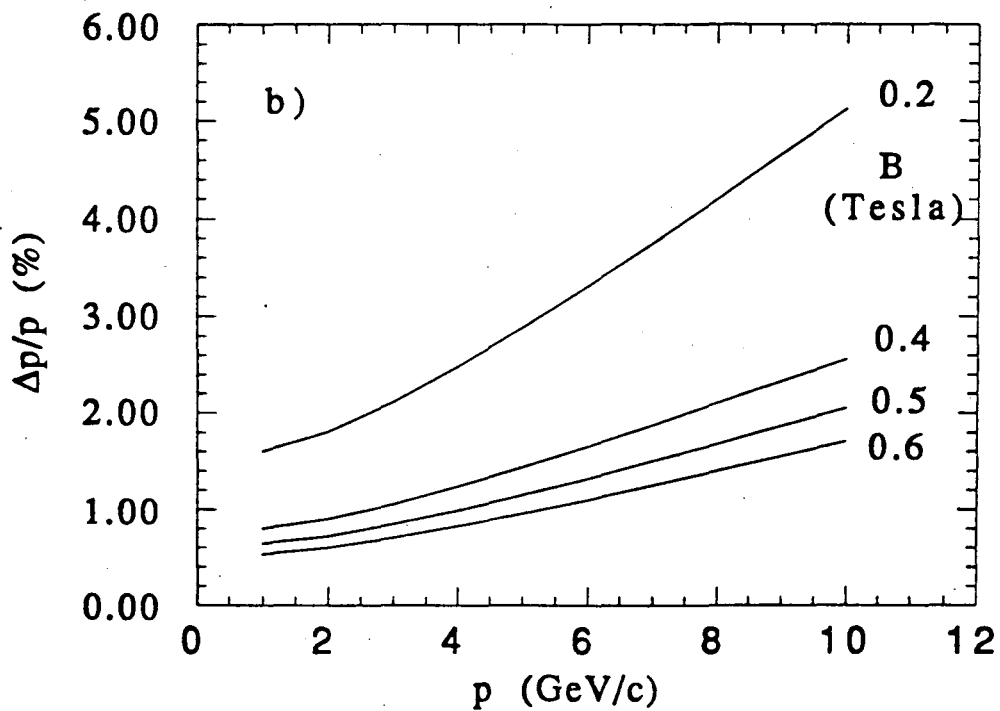
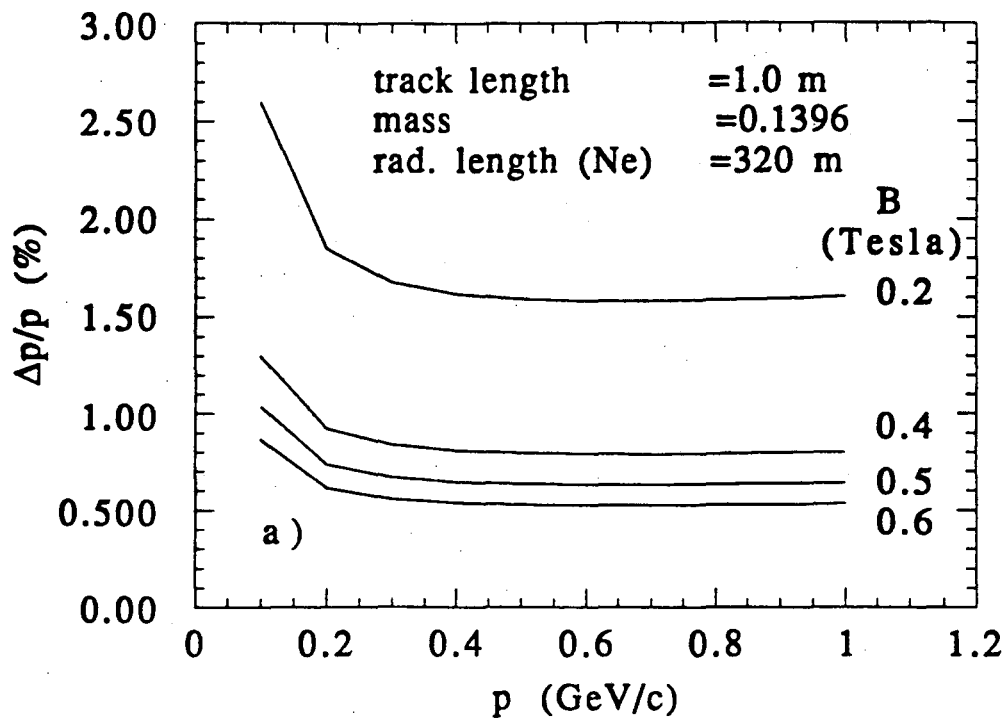
The gas inside the TPC is expected to be neon in order to reduce primary electron diffusion and multiple scattering in the TPC which dominates the momentum resolution at low momentum. The momentum resolution is displayed in Fig. 8a for the low momenta and Fig. 8b for the high momentum range of the experiment. These were calculated for the TPC using neon gas, without vertex determination and without the silicon vertex tracker. Knowledge of the vertex will improve the momentum determination. The momentum resolution at high momentum is dictated by the spatial resolution at the outer radius of the TPC.

The two-particle correlation analysis requires the highest two-track and momentum resolutions.

The momentum difference resolution Q for an idealized experiment has been calculated and appears in Fig. 4. A RHIC Detector R&D proposal has been submitted to determine the feasibility of a TPC with improved track-pair resolution at the outer radius, which is critical for measuring the largest pion source sizes ($\sim 30 \text{ fm}$) expected in central Au + Au collisions.

The 50 μsec drift time of the TPC limits the maximum interaction rate that the detector can withstand. At the expected luminosities of $2 \times 10^{26} \text{ cm}^{-2} \text{ s}^{-1}$ and $2 \times 10^{30} \text{ cm}^{-2} \text{ s}^{-1}$ for Au + Au and p + p interactions, respectively, the expected interaction rates were calculated. For Au + Au interactions, a rate of $2 \times 10^3 \text{ s}^{-1}$ and an average time between minimum bias interactions which is a factor of 10 longer than the drift time of the TPC are expected. The TPC can adequately measure events from Au + Au interactions at RHIC for up to an order of magnitude higher luminosity before events start to overlap during the drift time. When this occurs events from interactions other than the one triggering the readout of the TPC appear as tracks with the vertex displaced along the drift direction. Thus, only in the rare case when two central Au + Au events overlap in the 50 μsec drift time does it become prohibitive to disentangle tracks from independent events. For p + p interactions, a rate of $2 \times 10^5 \text{ s}^{-1}$ is expected and the average number of minimum bias p + p interactions registered during the drift (readout) time of the TPC, 50 μsec , is 10. Since minimum bias p + p events are mainly low multiplicity, leading particle events, only a fraction of these events will produce particles which even enter the TPC at midrapidity. In any case, since the TPC is designed to measure and reconstruct charged particle multiplicities of 3000 per event, a superposition of 10 minimum bias p + p events can be reconstructed easily from the TPC measurements, and the individual interaction vertices displaced along the drift direction can be determined. Therefore, the TPC is capable of measuring at the interaction rates expected at RHIC.

Momentum Resolution



8. Momentum resolution of the TPC for two ranges of momenta.

Table 3. Occupancy Factors in the TPC for $|\eta| \leq 1$

Radius (cm)	Occupancy (%)
50	15
100	4
150	1.8
200	1.0

The occupancy factors for the TPC as a function of radial distance have been calculated using the CERN GEANT detector simulation program for the highest multiplicities expected at RHIC. The primary particle distribution was generated using the Lund/FRITIOF nucleus-nucleus code⁴⁹ for 100 GeV/n colliding Au + Au beams at impact parameter $b = 0$. All primary and produced secondary particles were tracked through the TPC assuming the materials listed in Appendix 1. Assuming a 2

cm two track resolution in each direction at any point inside the TPC, the occupancy factors for the resulting 4 cm² lateral pixels at various radial distances are listed in Table 3. These occupancy factors are low enough so as not to impair the particle tracking efficiency of the TPC.

Table 4. Silicon Vertex Tracker

Inner radius	10 cm
Outer radius	20 cm
Length	50 cm
Total thickness	600 μ m
	$\sim 0.5\% L_T$
First layer of Strip Detector:	
Number of sections	8
Length of strips	6.25 cm
No. of strips per section	12,500
Pitch	50 μ m
Stereo angle	5 mrad
Pixel dimensions	50 μ m x 1 cm
Pixel area	0.5 mm ²
Cell occupancy	0.7 %
Double hit probability	2×10^{-5}
First layer of Pixel Detector:	
Number of pixels	300,000
Pixel area	1 mm ²
Cell occupancy	1.3 %
Double hit probability	10^{-4}

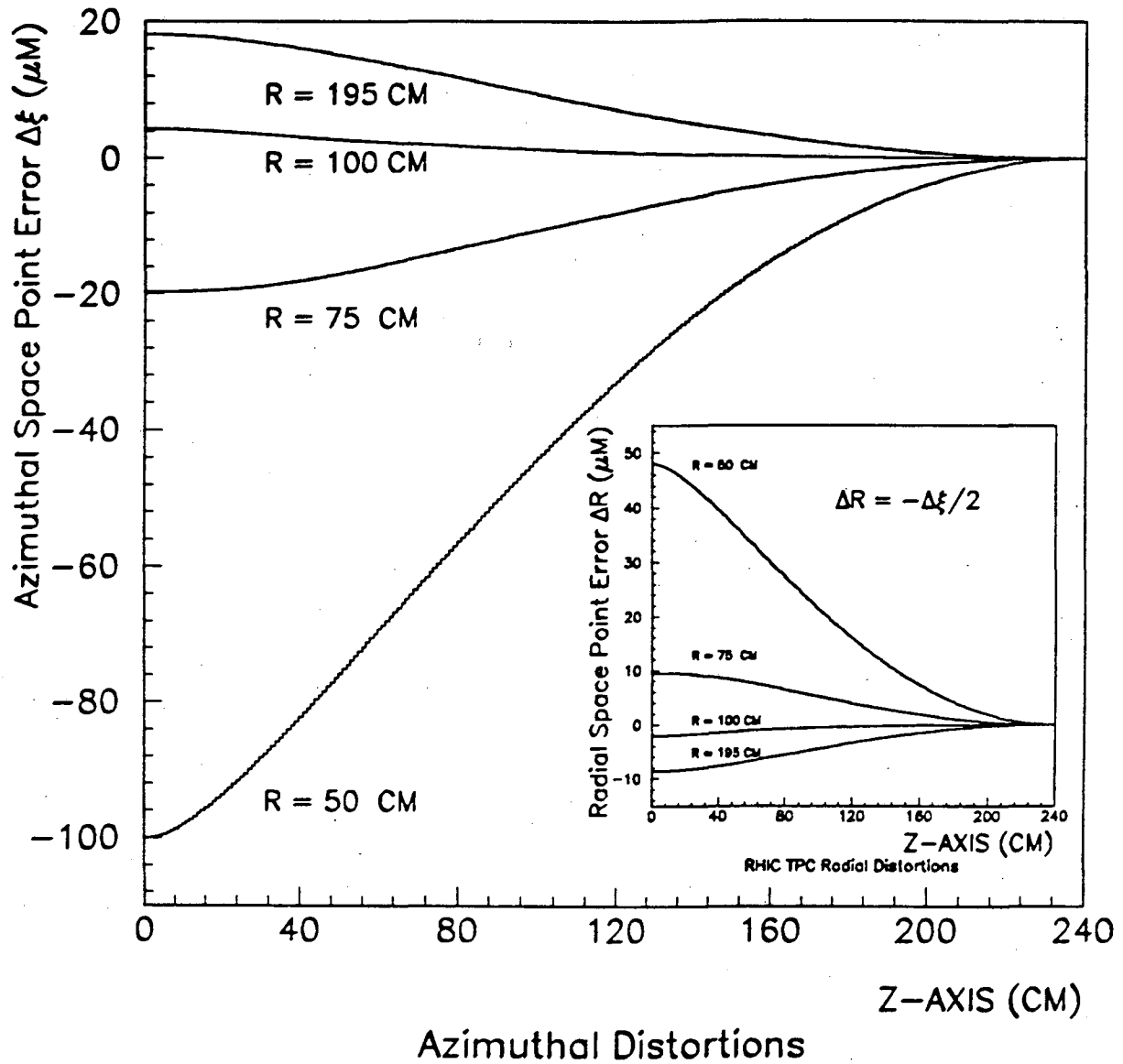
Considerable attention has been paid to possible distortions in the electric drift fields caused by positive ion space charge effects in the TPC. The use of a gating grid will eliminate positive ion feedback from the avalanche region near the sense wires. Detailed electrostatic calculations have been performed to ascertain the extent to which positive ion build-up from the primary ionization in the TPC, created by the large charged particle multiplicities at RHIC, may cause field distortions in the TPC. Displayed in Fig. 9 are the errors for space points along the azimuthal and radial directions as a function of the distance along the beam axis away from the detector center. For radial distances of 75 cm to 200 cm, the outer radius of the TPC, the errors are $< 20 \mu$ m in the azimuthal direction and $< 10 \mu$ m in the radial direction. These errors do not affect the momentum resolution of the TPC. The azimuthal and radial distortions reach maxima at the inner radius, 50 cm, of the TPC, with space point errors of 100 μ m and 48 μ m, respectively. Inclusion of this maximum error

for the first point along tracks does not degrade the resolution below that specified above. Even at a luminosity of $2 \times 10^{27} \text{ cm}^{-2} \text{ s}^{-1}$, a factor of ten higher than initially planned for RHIC, the TPC is not expected to have space charge problems when a low ionization potential gas such as neon is used.

D. Silicon Vertex Tracker (SVT)

The functions of the silicon vertex tracker (SVT), coupled with the TPC, are to locate the position of the primary interaction vertex to high accuracy, to improve the momentum resolution especially for high momentum tracks, and to locate secondary vertices to an accuracy better than

RHIC TPC Position Errors due to Space Charge



9. Results of electrostatic calculations showing the displacement errors due to space charge for points in space along the azimuthal and radial (insert) directions as a function of the distance along the beam axis z . The detector center is at $z = 0$. The TPC gas in the calculation is argon-methane (90:10) at STP. A luminosity of $2 \times 10^{26} \text{ cm}^{-2} \text{ s}^{-1}$ was assumed for simulated Au + Au collisions at RHIC.

100 μm . The SVT will be used to improve the overall tracking to meet requirements set by two-particle correlation measurements for particles with small momentum differences. The SVT must be able to provide three dimensional space points and tracking vectors with high spatial resolution, so that the tracks measured in the TPC can be linked to those in the SVT. To cover $|\eta| < 1$ the SVT will be located at a radius of approximately 0.1 m from the beam and have a length of 0.5 m, as shown in Fig. 7.

The design of the SVT depends upon developments in silicon detector technology.^{51,52} It should be cylindrical in shape and either a multilayer pixel detector or a multilayer strip detector made up of doublesided stereo layers. A list of the specifications for the SVT for both possibilities is presented in Table 4. The SVT must be of low mass so as to minimize secondary particle production, photon conversion, secondary interactions and multiple scattering. A RHIC Detector R&D proposal has been submitted for developing a multilayer silicon tracker of doublelayer strip detectors.

E. Time-of-Flight (TOF) Detector

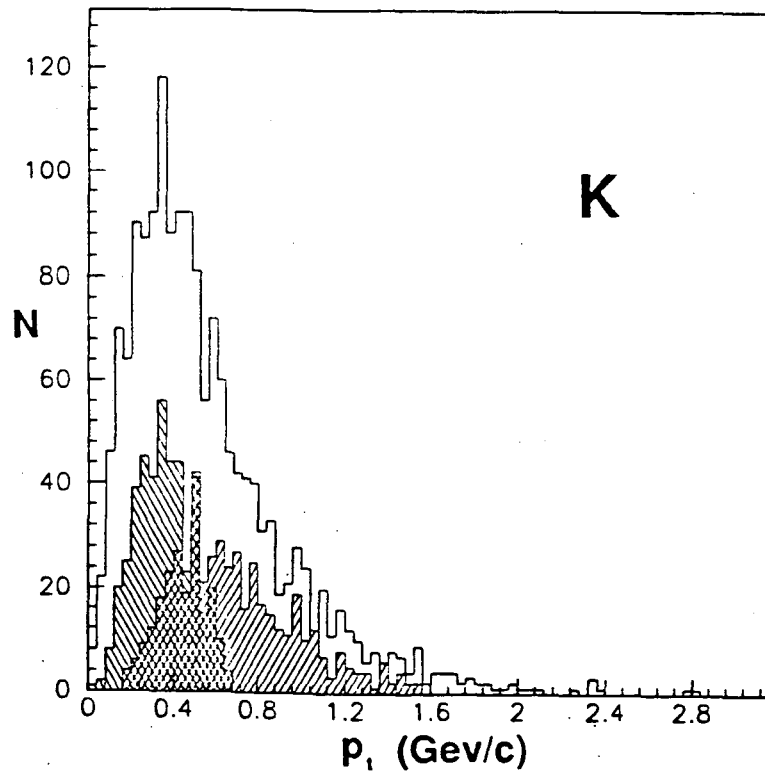
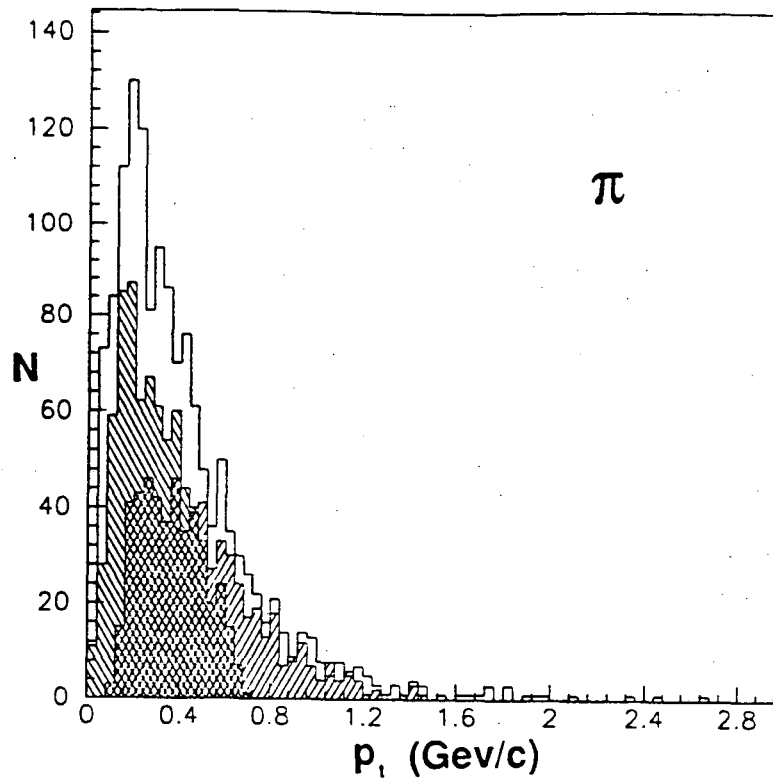
The particle identification capability of the TPC is mainly for momenta $p < 0.8 \text{ GeV}/c$. A TOF system is used to extend the particle identification to higher momenta. A summary of the specifications of the TOF system is provided in Table 5. The particle identification that can be achieved with the TPC - TOF system combination is displayed in Fig. 10. Plotted in Fig. 10 are the pion and kaon p_t distributions generated using Lund/FRITIOF and tracked using GEANT in the experiment as described above. The shaded regions represent particle identification using dE/dx techniques in the TPC and using TOF. The open histogram areas are those in which neither technique could identify the particles. Most of these particles in the open areas have either interacted or decayed in flight. At a distance of 2 m from the beam, the TOF system with a 6 cm^2 pixel size and 100,000 pixels has a maximum occupancy factor of 1.5% and a double hit probability of 2×10^{-4} . The high degree of segmentation is dictated by the need to match the TPC two-track resolution in order to identify particles nearby in momentum space for HBT correlation studies.

Table 5. Time-of-Flight Detector	
Radius	2 m
Area	60 m^2
Cell occupancy	1.5%
Pixel size	6 cm^2
Channels	100,000
Time resolution	< 100 psec
Channel dead-time	< 1 msec

The TOF system has not been designed. A TOF system that operates in the magnetic field is preferred. Due to the large number of channels, lower cost detector systems than those presently available must be developed. RHIC R&D proposals have been submitted to investigate the feasibility of developing low cost Pestov spark counters or silicon avalanche diodes for this purpose.

⁵¹ S. Parker, Nucl. Instr. Meth. A275 (1989) 494.

⁵² "SSC Detector R&D Proposal: Development of Technology for Pixel Vertex Detector," D. Nygren, spokesperson (1989).



10. Transverse momentum distribution, dn/dp_t , for charged pions (above) and kaons (below) from the primary interaction vertex generated by the Lund/FRITIOF nucleus-nucleus code and tracked through the experimental setup. The $\\\\\\\\$ region contains those particles identifiable with dE/dx measurements in the TPC. The $////$ region contains particles identified by TOF. The cross-hatched region has particles identified by both methods and the open region by neither. Most of the particles which are not identifiable and appear in the open region either interact or decay in flight.

F. Midrapidity Calorimeters

The purpose of the midrapidity calorimeters is to measure and trigger on high p_t jets and the transverse energy of events. The calorimeters will consist of separate electromagnetic and hadronic sections with a lateral segmentation of $\Delta\phi = 10^\circ$ and $\Delta\eta = 0.1$, for a total of 720 towers. The lateral segmentation may change after more extensive simulations are carried out. The inner diameter will be 2.5 m and outer diameter 3.8 m. Fig. 7 displays the calorimetry relative to the other detectors in the experiment. The necessity to precisely measure jet energies and transverse energy distributions at midrapidity suggests the use of a compensated calorimeter with a linear response down to low energies. Corrections to the calorimeter measurements for distortions of the trajectories of charged particles in the magnetic field will be made using the tracking data.

Hadronic

The hadronic calorimetry will consist of Pb/scintillator sandwich (1 cm Pb, 2 mm plastic scintillator) with energy resolution of approximately $0.35\text{--}0.40/\sqrt{E}$. The modules are designed to point towards the interaction vertex region and are 6 interaction lengths deep.

Electromagnetic

The design of the electromagnetic (EM) calorimeters has yet to be determined. It will be between 0.3 and 1.2 interaction lengths thick, depending on simulations of jet resolution and calorimeter response. The most straightforward choice for the calorimeter is to utilize the same Pb/scintillator sandwich structure used for the hadronic section. In practice, a compensated section with the same response as the hadronic section produces a system which is much easier to construct and calibrate than a high resolution EM section. The EM energy resolution is expected to be approximately $0.22/\sqrt{E}$.

The burden for good jet energy resolution rests on the EM calorimeter. It must operate in a significant background of low energy charged pions, whose shower profiles in sampling calorimeters are very similar to EM shower profiles. This charged pion background is strongly affected by the magnetic field, and must be taken into consideration in the simulations.

G. Intermediate Rapidity ($1 < |\eta| < 5$) Detectors

The region $|\eta| > 1$ is presently unspecified. An extension of the calorimetry to $|\eta| \sim 1.5 - 2$ is being considered to improve the definition of jets. Since jets are observed to spread energy over a region of pseudorapidity (η) and azimuthal angle (ϕ) of size approximately $\sqrt{(\Delta\eta)^2 + (\Delta\phi)^2} = 1$ about the direction of the jet, edge effects are reduced by calorimeter coverage extending beyond $|\eta| = 1$. For event characterization, full calorimeter coverage is preferred. Likewise, there are similar event characterization reasons for expanding the charged particle *multiplicity* coverage to include the region $1.7 < |\eta| < 5$. These possibilities are being studied in simulations.

H. Triggering

The triggering scheme is still being developed. A three level trigger is anticipated. The first level trigger will consist of decisions at the "hardware" level. Several parallel triggers are expected at this level: multiplicity, E_t , forward energy, total energy and various ratios of these quantities. First level decisions are made in less than a μsecond . The TPC readout and digitization of counters commence on this trigger. The second level trigger is decided in tens of $\mu\text{seconds}$. It could consist of topological configurations of interest from the detectors, such as

single jets, back-to-back jets, or fluctuations of various observables. The third level trigger operates on a time scale of milliseconds up to seconds. It should consist of trackfinding, momentum reconstruction, particle identification and thus data compression. The various parallel triggers will be prioritized such that triggers with the smallest cross sections can receive priority.

It may be possible to use the third level trigger to select high p_t hadrons as straight tracks in the TPC. However, to be able to trigger efficiently and quickly on high p_t hadrons, it is possible to use thin layers of fast-tracking detectors with high spatial resolution surrounding the TPC. This system could be constructed from straw tubes. This detector, in conjunction with the silicon vertex tracker or another high spatial resolution detector just inside the inner TPC radius, could be used to provide a fast trigger for straight high p_t tracks and also improve on the two-track and momentum resolutions stated above for the TPC alone. Simulations will be undertaken to address the efficiency of this type of triggering scheme in the background environment of the entire experiment.

I. Spectator Calorimeter

A spectator calorimeter to measure the forward energy at rapidities near that of the beam must be developed. This detector might be common to all experiments. The forward energy information from a spectator calorimeter can be correlated with the midrapidity calorimeters to characterize events by centrality in nucleus-nucleus collisions.

J. Time-of-Flight Start

Two radially segmented cones forming an array of slats of solid Cerenkov detectors will form the time-of-flight start. These cones will be centered on the beams on both sides of the collision diamond (Fig. 7). The Cerenkov slats will be angled $\sim 45^\circ$ away from the vertex to capture and totally internally reflect a fixed fraction of the produced light for high β particles. The pulse size in each slat gives the number of particles hitting it, providing a multiplicity count. The mean leading edge time of all the slats provides a tight (~ 50 ps) time-of-flight start, while the time difference between the two cones will provide a fast estimate of the vertex position to about one cm. Possible reaction plane information may be obtained from the azimuthal distribution in the slats. The position of the slats will be radially adjustable to maximize signal to noise, and to remove them from the beam at fill and dump times.

K. Data Acquisition

At present the maximum expected data acquisition rates for this experiment range from one central Au + Au interaction per second to ten minimum bias Au + Au interactions per second, limited by processing speeds and storage rates. The event size for central Au + Au collisions is expected to be 80 MB. After reduction by the average occupancy factor expected for the TPC (6%) this becomes 5 MB per event. Fast online analysis of the data to extract points in space along tracks can reduce the event size by a factor of 2 - 4. Any further large-scale reduction requires track-fitting. It is possible that with some developments in online data reduction and compression the data rate could be increased, as much as tenfold. A RHIC R&D proposal has been submitted to investigate this.

The goals of this experiment require data acquisition utilizing a range of projectiles (from protons to Au), available beam energies, and impact parameters. It is expected that longer data acquisition periods will be necessary for studies of jet production in p + p, p + Au, Au + Au and an intermediate mass system, than for measurements of the soft physics observables. However,

it should be realized that the data acquisition requirements of this experiment are inherently different from those of experiments which measure observables with small cross sections and require data accumulation with a fixed projectile and energy for as long as possible.

L. Cost Estimate of Experiment

The estimated total cost for the proposed experiment is \$35.4 M plus the cost of the time-of-flight system which is dependent upon R & D progress. An outline of the cost estimate is tabulated below.

Table 6. Cost Estimate		
Magnet		\$4.1 M
yoke	\$0.8 M	
coil and cryostat	\$2.5 M	
engineering	\$0.5 M	
support, misc.	\$0.3 M	
Silicon Vertex Tracker		\$3.0 M
Time-Projection Chamber		\$13.3 M
field cages	\$2.5 M	
sectors and support structure	\$2.6 M	
laser calibration system	\$0.7 M	
electronics	\$7.5 M	
Calorimeters		\$12.5 M
hadronic (6 L _I)	\$9.5 M	
electromagnetic (0.6 L _I)	\$3.0 M	
Computers		\$2.5 M
Time-of-Flight		?
Total		\$35.4 M
		plus Time-of-Flight

Acknowledgements

The authors wish to thank S.I Chase and D. Shy for significant contributions to various aspects of this Letter of Intent. We thank Y. Billawalla, H. Crawford, J. Engelage, M. Partlan, P. Seyboth, Y. Shao, L. Teitelbaum, H. Van Hecke, R. Welsh and W. Wenzel for participation in the development of this concept. Discussions with W. Carithers, W. Geist, N.K. Glendenning, B. Jacak, R. Kadel, T. Ludlam, S. Nagamiya, M. Shapiro, J. Siegrist, L. Van Hove and G. Young were very helpful and are gratefully acknowledged. The authors also wish to thank M. Gyulassy and X.N. Wang for many fruitful discussions and their continuing theoretical efforts in this field. This work was supported in part by the Director, Office of Energy Research, Division of Nuclear Physics of the Office of High Energy and Nuclear Physics of the U.S. Department of Energy under contract DE-AC03-76SF00098.

Appendix I: Table of Materials

Structure	Material	Thickness (cm)	$\frac{thk \cdot \rho}{L_r}$ (%)	$\frac{thk \cdot \rho}{\lambda_I}$ (%)
Beam Pipe	Be	0.10	0.28	0.24
Vertex 1	Si	0.020	0.21	0.044
Vertex 2	Si	0.020	0.21	0.044
Vertex 3	Si	0.020	0.21	0.044
Total Vertex			0.63	0.132
Gas R = 8 - 50 cm	He	42.0	0.008	0.01
TPC Gas Vessel	C	0.10	0.53	0.26
Mylar Insul.	C ₅ H ₄ O ₂	0.25	0.87	0.40
Total Vessel			1.40	0.66
Inner Field Cage	Al	0.03	0.34	0.08
Mylar	C ₅ H ₄ O ₂	0.19	0.66	0.31
Field Cage	Al	0.03	0.34	0.08
Total Field Cage			1.34	0.47
TPC Gas	Ne	150	0.47	0.14
Outer Field Cage	Al	0.10	1.13	0.27
Mylar	C ₅ H ₄ O ₂	0.23	0.80	0.37
Field Cage	Al	0.10	1.13	0.27
Total Field Cage			3.06	0.91
Mylar Insul.	C ₅ H ₄ O ₂	0.30	1.04	0.49
Coil & Cryostat	mostly Al	20.0	50	11
Calorimeter	Pb-Al-Scin.	175		
Return Yoke	Fe	12.5		

Appendix II: RHIC Detector R&D Proposals

Summary of Detector R&D

Several detector R&D projects are necessary for the success of this experiment.

One project, already funded, is to develop *Integrated TPC Electronics* which include preamp, shaper, analog storage and ADC in a single integrated circuit.

Development of high resolution ($\sigma \sim 100$ ps) time-of-flight detectors, which are inexpensive compared to the cost of photomultiplier tubes, is important when considering 100,000 channels of detectors. Possible operation of these TOF counters in a magnetic field has led to consideration of *Pestov Spark Counters* and *Silicon Avalanche Diodes* for development.

A project is underway to study the feasibility of a *High Track-Pair Resolution TPC* which uses a parallel plate avalanche readout with resistive mesh to increase the two-track resolution, possibly tenfold.

In order to be able to increase the data acquisition rate, *Online Data Compression* via track processing and analysis will be pursued.

The development of a vectoring *Silicon Vertex Tracker (SVT)* is necessary for this and possibly other RHIC experiments. Either a pixel tracker system or a multilayer strip detector with double-sided stereo layers will be developed.

The calorimetry must be designed and the *Calorimeter Readout* optimized for use in this experiment. Various readout techniques, for example the use of wavelength shifter bars or fiber optics, will be investigated.

For calibration of the TPC, a unique *3-D TPC Laser Calibration System*, utilizing time modulation of ultraviolet laser light to produce three-dimensional space points of ionization in the TPC, will be developed.

Read-out Electronics for the TPC Detector

A.A. Arthur, F. Bieser, B. Hearn, S. Kleinfelder, K. Lee,
J. Millaud, M. Nakamura, G. Rai, H.G. Ritter, H. Wieman, Y. Ye
Lawrence Berkeley Laboratory

We propose to develop a complete chain of highly integrated read-out electronics for the TPC detector described in this letter of intent. It is obvious that existing solutions (e.g. ALEPH) are not adequate for the some 150000 channels that need to be instrumented. It will be necessary to perform all the signal processing, digitization and multiplexing directly on the detector in order to reduce per channel cost and the amount of cabling necessary to read out the information. We will follow the approach chosen by the EOS TPC project, where the readout electronics on the detector consists of an integrated preamplifier, a hybrid shaping amplifier, an integrated switched capacitor array and a highly multiplexed ADC. Our goal is the production of an integrated circuit containing several channels of TPC read-out electronics. Each individual channel will consist of a preamplifier, a shaper and an analog store (switched capacitor array). We propose to proceed by developing and optimizing the individual components separately, using the same process for all three elements so that the integration can be done later. This effort is a continuation of the funded proposal "Highly integrated electronics for a TPC detector (RD-13)".

In addition to the design work, we will study the possibility of replacing or compensating the analog shaping in hardware with digital signal processing techniques. Feasibility tests will be performed using EOS TPC electronics which contains a digital signal processor. This work will be done by the physicists in the EOS TPC group and by electronics engineers. The outcome of this study will greatly influence the final design of the RHIC TPC electronics.

R&D for a Subhundred Picosecond TOF Detector

C.R. Gruhn
Lawrence Berkeley Laboratory

Relativistic Nuclear Collisions Group
Lawrence Berkeley Laboratory

Since this RHIC detector requires 100,000 channels of 100 ps TOF elements, the conventional approach of using photo tubes is prohibitively expensive. Thus, a modification to the Pestov spark TOF detector design is proposed. The Pestov spark detector relies on polymer production to control the spark via the Malter effect and at the same time limit the energy available to the spark. Variations of the design have been successfully achieved by controlling the energy going to the spark with resistive cathodes. These two approaches have been limited in terms of reliability and/or local dead time associated with the charging of the resistive surface.

A design study which avoids the spark but still uses the very high pressures and small drift distances is proposed. Drift gaps ranging from 100 microns to 1 mm in cylindrical and planar geometries would be used with gas mixtures at pressures of 10 to 100 atmospheres. The gain of the devices would be limited to a maximum of 10^7 charges in the avalanche. The gas choices would be an attempt to quench the avalanche and still maintain a fast transport. The geometrical arrangement of the electrodes would be such as to allow mean timing and impedance matched transmission of the signals to a fast preamplifier. The design will be constrained to allow large surface areas to be covered with fine granularity.

In order to facilitate this design work we propose constructing a high pressure gas detector facility which would enable fast turn around of data from tests and timely in feedback to the final detector designs. We are requesting funds here for such a facility to establish proof of principle of the above idea.

Design and Prototype Fabrication of Silicon Avalanche Diode Arrays for a Fast ($\sigma < 100$ ps) TOF Detector

A.S. Hirsch, N.T. Porile, R. Scharenberg, M.L. Tincknell,
Purdue University

G. Rai
Lawrence Berkeley Laboratory

This RHIC TOF system requires $\sim 10^5$ pixels each with 6 cm^2 area. We propose to test one cm^2 silicon avalanche diodes which could be produced in square arrays on silicon wafers ($25\text{-}100 \text{ cm}^2$ per wafer).

We would examine the time dispersion of commercially available large area ($5 \text{ mm} \times 5 \text{ mm}$) silicon avalanche photo diodes using minimum ionizing particles traversing the depletion region.

We would design and fabricate a number of diodes on a single wafer and evaluate the yields and the cost per wafer.

We would investigate the design of the auxiliary electronics and the integration of these circuits into a compact device.

We would commission design and fabrication of prototype arrays to establish manufacturability for large scale ($\sim 10^4$) wafer production.

Time Projection Chamber Readout Using A Resistive Mesh Cathode Parallel Plate Avalanche Geometry

David R. Nygren, Physics Division
Lawrence Berkeley Laboratory

Relativistic Nuclear Collisions Group, Nuclear Science Division
Lawrence Berkeley Laboratory

A. Breskin, R. Chechik, Z. Fraenkel, A. Shor, and I. Tserruya
Weizmann Institute of Science

The use of a Parallel Plate Avalanche Detector (PPAD) as the readout for a Time Projection Chamber is discussed from the perspective of suppressing undesirable discharges characteristic of this geometry. By using a suitably resistive mesh to define the transition from the TPC drift region to the amplification region, in place of the conventional metallic electrode, complete suppression of sparking may be obtained. Successful realization of the PPAD readout geometry with resistive mesh will improve the track pair resolution performance of the TPC substantially, increasing the attractiveness of the TPC technique for many elementary particle physics and relativistic heavy ion physics applications.

In a high track density environment, the natural size of anode pads could be on the order of 1 mm², leading to electronic channel densities of similar scale: 10⁶/m². If tracks are concentrated in a specific direction, then long pads can be used without loss of resolution, reducing the channel count substantially. With the advent of VLSI custom IC design expertise within the nuclear and elementary particle physics communities, large channel counts may be feasible. The most obvious application for this development would be for RHIC, where secondary track multiplicities reach into the thousands.

Development Program

A modest program of effort should be sufficient to exploit this concept. The cost would be for manpower estimated to be one person's time and a similar budget level for a technician, materials and shop time.

Data Compression and Preprocessing

Fred Bieser and Charles McParland
Lawrence Berkeley Laboratory

Relativistic Nuclear Collisions Group
Lawrence Berkeley Laboratory

We have based this proposal on the following premises for the RHIC TPC:

- 1) Detector-mounted circuitry will produce approximately 80 MBytes of data per event which will be received over optical fibers.
- 2) At 100 Mbits/sec/fiber there will be 10 receiver channels.
- 3) Pedestal subtraction and zero suppression can be done during data reception by simple state machines (as done on the Berkeley EOS TPC), resulting in a reduction of the data by approximately 90%.
- 4) Making gain corrections and extracting centroids and pulse-heights will not compress the data set very much further but is a necessary step in track reconstruction and, as such, should be done as rapidly as possible.

On the EOS TPC we are using *integer* DSP's to do gain correction, IIR pulse shape filtering, and secondary zero suppression. The off-line processing of the data (beginning with centroid finding) involves the use of logarithms and calculations of considerable dynamic range.

Therefore, we propose to:

- 1) Investigate the availability of *floating point* DSP hardware (and associated development tools) which might be appropriate for rapid centroid finding.
- 2) Select one (or more) device(s), build breadboard circuits, and make some performance tests.
- 3) Consider the architecture necessary to handle a very high data transfer rate from multiple DSP's to one of several (parallel) processors for track reconstruction.
- 4) Survey the market for commercial board-level processors that could be employed to perform track reconstruction *on line* and thereby reduce the data set to a modest 40 KBytes/event before taping.

Silicon Tracking Detector for RHIC

Grazyna Odyniec

Lawrence Berkeley Laboratory

Relativistic Nuclear Collisions Group

Lawrence Berkeley Laboratory

Due to the physics motivations outlined in this Letter of Intent and the expected complexity of events at RHIC, it is clear that the experimental setup requires a high precision tracking detector positioned close to the interaction region. Addition of a silicon vertex detector (SVX) to the apparatus would serve two purposes:

1. High-precision primary vertex determination which can improve the main vertex position accuracy by a factor of 10 compared with the position obtained from the TPC alone.

2. Improvement of momentum determination of measured particles. Addition of points from the SVX with an accuracy of 10 μm to the track trajectory determined from the TPC with a 100 μm accuracy decreases uncertainties in the momentum determination on the average by a factor of 5.

This is still not sufficient in view of the physics goals. Therefore we propose a Silicon Vertex Tracker (SVT), based on vector tracking schemes using information from multilayer silicon detectors, which provides 3-dimensional description of the measured track. In addition to the information obtained from the SVX (1. and 2.), the SVT will allow:

3. Determination of secondary vertices with high accuracy.

4. Improvement of momentum determination for non-primary vertex tracks.

The detector will be based on technology which has been proven to work in a physics experiment: Si strip detectors with capacitive charge division readout (5 μm) combined with LSI readout electronics allowing a high degree of multiplexing at the detectors. We envision a program devoted to exploring and understanding the most efficient design for application to the RHIC environment. The entire R&D effort will be divided into two categories:

1. Monte Carlo studies to evaluate the tracking efficiency and its dependence on design parameters. A comparison of the resolution of secondary vertices from the primary vertex using the TPC alone and with addition of the SVT will be undertaken. In addition, improvements in momentum measurements will be quantified.

2. Lab tests for visual inspection of silicon detectors under a microscope, strip tests with calibrating pulses using probe stations, "stand alone" electronics tests, and tests of the complete detector with calibrating pulses and laser beams after connecting detectors with front-end electronics. The main goal of the first year of R&D study is to determine a suitable configuration of a multilayer system of detectors appropriate for RHIC. Year 1991/1992 will be dedicated to measurements of the performance characteristics of the prototype. The next step (1992/1993) is the design (simulations, designing and prototyping) of the full scale detector. That will include significant contributions from the engineering staff.

Calorimeter Research and Development

K.L. Wolf, A.D. Chacon, R. Erkert, and J. Shoemaker
Texas A&M University

Introduction

Calorimetry for mid-rapidity RHIC experiments must meet some extended criteria compared to past applications, reflecting the low energies and high multiplicities in heavy-ion collisions. The requirements for the central hadronic calorimeter are defined in the present proposal, and the feasibility of a finely segmented electromagnetic device is under study. Sampling calorimeters utilize cheap construction materials up to the point of the electronic readout, and usually provide the more cost effective solution compared to the use of homogeneous calorimeters for electromagnetic energy. Lead glass Cherenkov devices have the advantage of blind response to low energy charged pions, and barium fluoride provides a fast timing capability. The disadvantages of the latter two types of detectors are costly scintillator and expensive quartz windowed phototubes, accompanied by a poor response for hadrons, in the homogeneous calorimeter itself and in the subsequent sampling hadronic calorimeters.

Proposed Development

Emphasis is placed on improved readout techniques with an integrated approach to eliminate conventional phototubes and to simplify engineering and construction techniques. A major cost for a hadronic calorimeter is in materials. Readout cost for 760 towers here become more significant when some longitudinal segmentation is required, as appears to be the case at RHIC. A compact readout scheme allows simpler design, lower costs for construction and electronics, and better performance through the elimination of dead regions. The specific proposal is for development of the wavelength shifting optical fiber method for a hadronic calorimeter surrounding a large TPC. A somewhat different fiber-scintillator coupling is needed than has been used in the past. Estimates indicate a 20% savings in the overall cost for construction of a hadronic calorimeter, compared to the use of conventional WLS bars and light guides.

Research on electromagnetic calorimetry may be outlined:

- 1) Calculations must be performed in a simulated RHIC environment, and with the magnetic field and geometry of the TPC. A parameterized shower code will be used, which includes recently generated low energy data from the Participant Calorimeter project. The use of sampling and homogeneous calorimeters and the feasibility of neutral pion reconstruction will be investigated.

- 2) Development of the WLS fiber optic method for sampling calorimeters will be conducted. Other compact readout schemes will be considered, with the main effort on the design of a practical, cost effective readout technique which eliminates photomultiplier tubes.

Laser Generated Ionized Tracks with Periodic Spatial Structure for Calibration of the TPC Detector

H. Wieman, H. Matis, D. Olson, G. Rai, H.G. Ritter, Y. Shao and C. Wieman
Lawrence Berkeley Laboratory

Introduction

We propose developing an improved laser system for the geometric calibration of the RHIC solenoidal TPC. Currently, pulsed UV laser beams are being used to create straight line ionized tracks through TPC detectors to establish reference lines for geometric calibration.¹ Our proposed system is a significant improvement over this approach because it would create fixed reference points of enhanced ionization along each laser track. This would provide a complete three dimensional reference grid within the detector volume. With present techniques intersecting laser beams must be used to establish reference points in the gas volume. The number of these crossing points is normally severely limited by the complexity of the optics and the availability of access into the gas volume. For this reason TPC designs have had to compromise full volume calibration coverage. With the new approach the volume could be completely referenced with parallel laser beams entering from one plane of the detector volume.

In the past, without this method of calibration, TPC designs have had to provide extremely precise electric and magnetic fields. This has required great expense in both effort and money, and in some cases has not been entirely successful.² In these cases a fully three dimensional laser point reference system would have either directly solved the problem or at least greatly simplified it's correction.

Proposed Method

Our approach would use a frequency quadrupled beam (266 nm wave length) from a Nd:YAG laser that has a 1 GHz amplitude modulation. The beam would enter the gas volume and be reflected back on itself. The ionization is quadratic in beam intensity (two photon process)³ so enhanced ionization will occur at the points in space where pulses traveling in opposite directions overlap, i.e. every 15 cm in the active gas volume. (A similar effect with localized enhancement of fluorescence is observed in non-linear fluorescing materials. The length of the enhanced fluorescence region, where the pulses overlap, is routinely used to measure the width of the laser pulse.)

Development of a test system will require a Q switched Nd:YAG laser, equipped with injection seeding to smooth the random time structure, a commercial 1 GHz modulator, two frequency doubling crystals and miscellaneous optical components. Total hardware costs are 88 K\$.

¹ H. Wieman, HISS TPC Note #140,31-Oct-89. "The ALEPH Handbook 1989", section 9 "Laser Calibration Systems", p V.48-V.53, CERN, ALEPH 89-77, NOTE 89-03, 28 April 1989.

² M. Iwasaki, R.J. Madaras, D.R. Nygren, G.T. Przybylski and R.R. Sauerwien, Time Projection Chamber Workshop, TRIUMPF, Vancouver, B.C., Canada, AIP Conf. Proc. 108 (1983) 214. W. Mueller (GSI) Private Communication. W. Love (BNL) Private Communication.

³ G. Hubricht, K. Kleinknecht, E. Muller, D. Pollmann, K. Schmitz, C. Sturzl, ALEPH-NOTE 154, 26.11.1985, (1985). K.W.D. Ledingham, C. Raine, K.M. Smith, M.H.C. Smyth, D.T. Stewart, M.Towrie and C.M. Houston, Nucl. Instr. and Meth. in Phys. Res., A241, 441 (1985). A. Bamberger, R. Isele, J. Schlupmann and M. Stegle, Nucl. Instr. and Meth. in Phys. Res A251, 67 (1986).

LAWRENCE BERKELEY LABORATORY
UNIVERSITY OF CALIFORNIA
INFORMATION RESOURCES DEPARTMENT
BERKELEY, CALIFORNIA 94720